JOURNAL OF AGRICULTURAL AND FOOD CHEMISTRY

Agricultural and Environmental Chemistry

The interaction between TaNOX7 and TaCDPK13 Contributes to Plant Fertility and Drought Tolerance by Regulating ROS Production

Chun-Hong Hu, Qing-Dong Zeng, Li Tai, Bin-Bin Li, Peng-Peng Zhang, Xiu-Min Nie, Peng-Qi Wang, Wen-Ting Liu, Wen-Qiang Li, Zhensheng Kang, Dejun Han, and Kun-ming Chen

J. Agric. Food Chem., **Just Accepted Manuscript** • DOI: 10.1021/acs.jafc.0c02146 • Publication Date (Web): 18 Jun 2020

The interaction between TaNOX7 and TaCDPK13 Contributes to Plant Fertility and Drought Tolerance by Regulating ROS Production

Chun-Hong Hu[1, 2†], Qing-Dong Zeng[3†], Li Tai[1], Bin-Bin Li[1], Peng-Peng Zhang[1], Xiu-Min Nie[1], Peng-Qi Wang[1], Wen-Ting Liu[1], Wen-Qiang Li[1], Zhen-Sheng Kang[4], De-Jun Han[3*], Kun-Ming Chen[1*]

[1], State Key Laboratory of Crop Stress Biology in Arid Areas, College of Life Sciences, Northwest A&F University, Yangling 712100, Shaanxi, P. R. China.

[2], College of Life Science and Agronomy, Zhoukou Normal University, Zhoukou 466000, Henan, P. R. China.

[3], State Key Laboratory of Crop Stress Biology in Arid Areas, College of Agronomy, Northwest A&F University, Yangling 712100, Shaanxi, P. R. China.

[4], State Key Laboratory of Crop Stress Biology in Arid Areas, College of Plant Protection , Northwest A&F University, Yangling 712100, Shaanxi, P. R. China.

[†], These authors contributed equally to this work.

*Correspondence author:

De-Jun Han

State Key Laboratory of Crop Stress Biology in Arid Areas, College of Agronomy, Northwest A&F University, Yangling 712100, Shaanxi, P. R. China.

Email: handj@nwafu.edu.cn

Kun-Ming Chen

State Key Laboratory of Crop Stress Biology in Arid Area/College of Life Sciences, Northwest A&F University, Yangling 712100, Shaanxi, China.

Tel.: +86-29-8703-1358; Fax: +86-29-8709-2262.

Email: kunmingchen@nwsuaf.edu.cn; kunmingchen@163.com.cn

E-mail addresses of authors: Chun-Hong Hu, ourcarrot@163.com; Qing-Dong Zeng, zengqd@nwafu.edu.cn; Li Tai, taily@nwafu.edu.cn; Bin-Bin Li, libinbin8754@sina.cn; Peng-Peng Zhang, 15256849763@163.com; Xiu-Min Nie, 2068515584@qq.com; Peng-Qi Wang, wangpengqi@nwafu.edu.cn; Wen-Ting Liu, lwt1635@yahoo.com; Wen-Qiang Li, wqli@nwsuaf.edu.cn; Zhen-Sheng Kang, kangzs@nwsuaf.edu.cn; De-Jun Han, handj@nwafu.edu.cn; Kun-Ming Chen, Kunmingchen@nwsuaf.edu.cn

ABSTRACT

Reactive oxygen species (ROS) homeostasis is critical for both physiological processes and stress responses of plants. NADPH oxidases (NOXs) are the key producers of ROS in plants. However, their functions in ROS homeostasis and plant growth regulation in wheat (*Triticum aestivum*) are little investigated. Here, we cloned and characterized a NOX isoform TaNOX7 in wheat. Overexpression of *TaNOX7* in rice led to enhanced root length, ROS production, drought tolerance as well as bigger panicles and higher yield, but shorter growth period duration. Further results indicate that TaCDPK13, a member of calcium-dependent protein kinases (CDPKs), can directly interact with TaNOX7 and enhance ROS production in plants. These results demonstrate that TaNOX7 plays crucial roles in wheat development, fertility, and drought tolerance via interaction with TaCDPK13, which may act as upstream regulator of TaNOX7 to regulate ROS production in wheat.

KEYWORDS: Wheat (*Triticum aestivum*), ROS, TaNOX7, TaCDPK13, fertility, drought tolerance

INTRODUCTION

Reactive oxygen species (ROS), such as superoxide anion radical (O_2^-) and hydrogen peroxide (H_2O_2), are essential in developmental processes and biotic/abiotic stress responses as signal molecules in plants.[1, 2] Although there are various ROS-generating pathways, the plasma membrane NADPH oxidases (NOXs), also named after respiratory burst oxidase homologs (RBOHs), are considered to be the key enzymes for apoplastic ROS production of plants under both normal and stress conditions.[3]

Increasing evidences have reported that NOXs/RBOHs participate in diverse biological processes by regulating their activity of ROS production. For example, in *Arabidopsis*, AtRbohB participates in seed after ripening,[4] AtRbohC (RHD2) modulates root hair formation and root-hair-cell growth,[5] whereas AtRbohD and AtRbohF not only regulate the immune response[6] and salt stress tolerance[7] but also function in jasmonic acid (JA)-induced gene expression.[8] Furthermore, it was reported that AtRbohD participates in abscisic acid (ABA)-mediated ROS production and stomatal closure,[9] lignin assembly,[10] and endosperm development.[11] In addition, AtRbohE regulates tapetal programmed cell death (PCD) and pollen development by interfering with the temporal ROS pattern;[12] AtRbohH/J also function in pollen tube development.[13] Recently, OeRbohh, a *Olea Europaea* NOX, was reported involving in the control of pollen germination and pollen tube elongation.[14] In rice, three NOXs, namely OsRbohA, OsRbohB, and OsRbohE, were found involving in immune response,[15, 16] and OsRbohA also plays a crucial role in drought-stress tolerance.[17] Later, OsRbohH was found to modulate the aerenchyma formation in roots[2] and OsNOX3 was reported to regulate root hair initiation and elongation.[18] Moreover, two maize NOXs, ZmRbohH and ROOTHAIRLESS5, were reported functioning in root development.[19, 20] Two *Pyrus bretschneideri* NOXs, PbRbohA/D might play an important role in the lignification of pear stone cells.[21] While, a *Medicago truncatula* NOX, MtRbohA, could be stimulated by hypoxia and which would, in turn, lead to the regulation of nodule functioning.[22] Our previous study found that there are at least 15 NOX/RBOH homologs in wheat, playing the vital but diversity roles in both the plant growth regulation and stress responses.[23]

It has been well known that ROS play dual roles in plants. They not only lead to programmed cell death by damaging the cellular components as deleterious factors under higher level, but are

also necessary for plant development and tolerance to different biotic and abiotic stresses acting as signal molecules under lower accumulation.[24, 25] Therefore, there must be a ROS threshold in plant survival. As thus, maintaining ROS homeostasis is particularly important to ensure normal physiological processes of plants, in which the mechanism of tightly regulating NOX activity is the pivotal problem. Numerous studies have highlighted the regulation of NOXs/RBOHs expression and activity in plants. For instance, four WRKY transcription factors, including WRKY8 phosphorylated by mitogen-activated protein kinases (MAPKs), can bind to the W-box element of the *NbRbohB* promoter and positively modulate the transcriptional levels of the *NbRbohB* gene;[26] ETHYLENE RESPONSE FACTOR 74 (ERF74) directly binds to the promoter of *AtRbohD* and activates its expression under different abiotic stresses.[27] A MAP4 kinase SIK1 was reported to enhance ROS production for defense in *Arabidopsis* by binding to and phosphorylating AtRbohD.[28] Ca^{2+} as signal molecular binds to the EF-hand region of AtRbohD, in which the conformational change in the EF-hand region induced a direct phosphorylation and synergistically activated the ROS producing activity of AtRbohD.[29] In addition, it was found that the cold-inducible protein AtSRC2 can activate AtRbohF for ROS production in a Ca^{2+}-dependent manner.[30] The receptor-like cytoplasmic kinase BIK1 not only specifically phosphorylates AtRbohD but also positively adjusts the flg22-induced increase of cytosolic calcium, both of which control the flg22-induced ROS production and the stomatal defense.[31] Furthermore, Ca^{2+} and phosphorylation treatments can induce the faster diffusion and clustering of AtRbohD at the plasma membrane, where clathrin and membrane microdomains synergistically affect the endocytosis of AtRbohD and thereby control the activity of the protein.[32] Moreover, phosphatidic acid (PA) was found regulating NADPH oxidase activity and ROS production during the ABA-mediated stomatal closure.[9] In rice, OsRac1, a

106 Rac/Rop GTPase, can directly activate OsRbohB/H for ROS generation to response to pathogen
107 infection[16] and Ca^{2+} plays a dual role (positive and negative) in regulating NOX activity and the
108 interaction between Racs and RBOHs.[33] In animals, Hace1, acting as the negative regulator of
109 NADPH oxidase, can bind to and ubiquitylate Rac1 to degrade the Rac1-NOXA1 complex, thus
110 blocking ROS generation.[34] These results indicate that NOX/RBOH-mediated ROS production
111 plays vital roles in plant development and the activity of the enzymes is subtly controlled by many
112 important intracellular signaling factors.[35]

113 As the primary sensors of Ca^{2+}, calcium-dependent protein kinases (CDPKs) are also
114 implicated in the regulation of NOX activity in plants. For example, StCDPK5 directly activates
115 StRbohB by phosphorylation in a calcium-dependent manner and regulates the oxidative burst for
116 defense responses to pathogens;[36] AtCPK5 phosphorylates AtRbohD and enhances ROS production
117 for defense responses and bacterial resistance;[37] MtCDPK5 can directly phosphorylate MtRbohB,
118 MtRbohC and MtRbohD, which triggered immune responses to regulate rhizobial colonization in
119 symbiotic cells of *Medicago truncatula*.[38] However, the regulatory mechanism and biological
120 significance of CDPKs in the regulation of NOX activity are still under investigation.

121 Wheat (*Triticum aestivum*) is a worldwide staple crop, necessitating a clear deciphering of its
122 developmental characteristics and stress tolerance mechanisms. However, up to now, only two NOX
123 genes of wheat were reported to be sensitive to brown rust infection.[39] Although at least 15 NOX
124 homologs were identified in wheat and their tissue and inducible expression patterns were
125 uncovered systematically,[23] the functions of wheat NOX family genes and their regulatory
126 mechanisms in both plant growth regulation and stress tolerance are still of largely elusive. In this
127 study, we firstly cloned a NOX homolog (TaNOX7) in wheat and investigated its biological

functions by employing a series of transgenic plants. The results obtained here show that TaNOX7, as a key producer of ROS, plays a vital role in plant development, fertility and drought tolerance. It directly interacts with TaCDPK13, a member of CDPKs, to regulate the ROS production of the plants, and therefore contributes to the plant growth regulation and drought tolerance. More interestingly, overexpression of *TaNOX7* in rice greatly improved the yielding traits with reduced growth duration period, implying that TaNOX7 is a well target to the improvement of fertility and stress tolerance of plants by molecular breeding.

MATERIALS AND METHODS

Plant materials and growth conditions

Wheat (*Triticum aestivum cv. Chinese Spring*) seedlings growing in field were harvested used for the gene expression profiles analysis and cloning. The AtRbohD-knockout mutant, *atrbohd*, which was isolated from an *Arabidopsis thaliana* T-DNA insertion mutant line N673320, was used for drought stress treatment or transgenic plant generation. A rice *OsNOX1* (*OsRbohB*)-knockout mutant, *osnox1*, which was screened from a rice Tos17 insertion mutant line NF5029_0_501_1A, was used to make callus for transgenic plant generation. Moreover, the wheat tissues, namely roots, flag leaves, and young spikes from inflorescence emergence stage of 100 varieties grown in field were harvested for transcriptional sequencing. The detailed information about the 100 wheat varieties, plant growth conditions, as well as the calculation standard for agronomic traits, refers to supplementary material SI and .

Transcriptome sequencing and data analysis

Total RNA of the roots, flag leaves and spikes from 100 varieties of wheat at inflorescence emergence stage, was extracted and broken into small fragments. Then the small fragments were

reversed transcription into cDNA. After end repair and add adapter, they were sequenced on Novaseq (Illumina, San Diego, USA, PE150) according to the manufacturer's standard protocols with 350 bp insert size. The clean reads were mapped against wheat genome (IWGSC ref V1)[1] using Hisat2 (version 2.1.0)[2] with default parameters. Then transcript was quantitative with StringTie[3] (version 1.3.5 stringtie -e -B -G). At last, the Transcripts per million reads (TPM) information for each sample was extracted, and Kruskal-Wallis test among genes was carried out with the function of stat_compare_means in R package ggpubr (R 3.6.3). The detailed information for 100 varieties of wheat are shown in Table S1.

mRNA isolation and RT-PCR

For the analysis of gene tissue-specific expression profiles, total RNA was extracted in the different samples from wheat cv. Chinese spring grown in field using RNAiso TM Plus kit (Takara, Dalian, China) and treated with RNase-free DNase I (Takara). The analysis of the tissue-specific expression profiles and coexpression relationship of *TaNOX7* and *TaCDPKs* genes were performed with the UltraSYBR Mixture (Kangwei, Beijing, China) with *TaActin1* (AB181991.1) and *TaGAPDH1* (ABS59297.1) as the internal transcript level controls. The detailed information for the genes, experiment performance and the primer sequences are shown in supplementary material SI and Table S2/3, respectively.

Subcellular localization analysis

The subcellular location of TaNOX7 was performed using an *Agrobacterium*-mediated instantaneous transformation system.[43] The AtCBL1n::MCherry construct was used as the marker for plasma membrane protein localization.[44] The methods in details refer to supplementary material

SI.

Transformation of plants

The coding region of *TaNOX7* and its promoter sequence named *TaNOX7pro* were all amplified for the expression vector construction using their primer-specific oligonucleotides. The vectors of pCAMBIA1301-35S-TaNOX7 and pCAMBIA1301-TaNOX7pro-GUS were transferred into calli obtained from the rice cultivar Nipponbare and the *osnox1* mutant, according to an *Agrobacterium*-mediated transformation method.[45] *TaNOX7* transgenic lines on *Arabidopsis thaliana* (Col-0, wild type) and an *AtRbohD*-knockout mutant *atrbohd* were also generated according to a method described previously.[46] The detailed information for transgenic plant generation and the specific primer sequences refer to supplementary material SI and Table S3, respectively.

Detection of ROS production

The histochemical analysis for H_2O_2 and O_2^- accumulation in plant tissues were conducted by 3, 3′-Diaminobenzidine (DAB) and Nitrotetrazolium blue chloride (NBT) staining, respectively, according to the previous described method.[47, 48] In addition, ROS production in root tips was visualized via fluorescence of 2, 7-dichlorodihydrofluorescein diacetate acetyl ester (H_2DCFDA). The H_2O_2 content in the samples was detected with the protocol of the Hydrogen Peroxide Assay Kit (Beyotime R technology, Shanghai, China), whereas the content of O_2^- were detected with the hydroxylamine oxidation method.[49] At same time, the O_2^- production rate in the rice transgenic lines was also detected with the sodium, 3'-[1-[phenylaminocarbonyl]-3, 4-tetrazolium]-bis (4-methoxy-6-nitro) benzenesulfonic acid hydrate (XTT) method as the described previously.[50] The

194 methods in details refer to supplementary material SI.

195

196 **GUS staining for the tissue/organ specific expression of *TaNOX7***

197 To examine the tissue/organ-expression specificity of *TaNOX7*, the GUS staining system was
198 employed as the described previously [51] with some modifications. The method of GUS staining in
199 details refers to supplementary material SI.

200

201 **Examination of plant stress tolerance**

202 The full and mildew free seeds of transgenic rice were selected and immersed into deionized water
203 at 37 ℃ for 48 h. After soaking enough water for germination, the seeds were put into 4% agar
204 including 1.0 μM H_2O_2 for 4 days, then were transferred into Hoagland's nutrient solution
205 containing 0.5 μM H_2O_2 and cultivated for 3 days. The phenotypes of the seeds geminating progress
206 were photographed and the germinating rate was recorded. At the same time, the length of roots and
207 numbers of adventitious roots were measured after the H_2O_2 treatment.

208 To examine the drought tolerance of transgenic plants, the seedlings cultivated with soil in pots
209 for one month were subjected to drought stress treatment by withholding water. After treated for 15
210 days, the plants were rewatered for 10 days and then the survival rates for the different plant lines
211 were recorded. Three biological experiments were performed and at least 50 plants were used for
212 the calculation. The water lose rate (WLR) was also assessed as the described previously[52] with
213 slight modifications. At the four-leaf stage, the third fully expanded leaves of the transgenic rice
214 plants were cut and their fresh weights (FW) were recorded immediately. The leaves were left on
215 filter paper in dry dishes in a growth chamber with a constant temperature of 23~25 ℃ and a relative

humidity of 40~60%. The leaves were weighed every 30 min ($W_{30\ min}$), and then the WLR for certain time points was calculated using the following formula: WLR %=[(FW-$W_{30\ min}$) /FW] *100. At least 6 leaves from different plants for each line were used for the analysis.

Firefly luciferase complementation imaging (LCI) assay

In order to verify the interaction between TaNOX7 and TaCDPK13, the firefly luciferase (LUC) complementation imaging (LCI) assay was performed according to a method.[53] First, we constructed the expression vectors TaCDPK13-cLUC and TaNOX7-nLUC, and transformed them into *Nicotianna benthamiana* leaves by an *Agrobacterium*-mediated transient transform method.[45] After inoculated 2 or 3 days, the chemilluminescence images and the fluorescence intensity profiles were all taken by a plant living imaging system (Lumazone Pylon2048B, Princeton, US). The detailed information refers to supplementary material SI and Table S3.

Bimolecular fluorescence complementation (BiFC) assay

Bimolecular fluorescence complementation (BiFC) assay was performed according to the method described by Walter and others.[54] The coding regions of *TaCDPK13* genes were cloned into pSPYNE vector with the N-terminal fragment of the yellow fluorescent protein (nYFP) and *TaNOX7* was cloned into pSPYCE vector with the C-terminal fragment of the yellow fluorescent protein (cYFP). Then, the *Agrobacterium*-mediated transient transform method[45] was used to transiently co-express TaNOX7-cYFP and TaCDPK13-nYFP in *Nicotianna benthamiana* leaves. The fluorescence visualization in leaves was observed with a confocal microscope (A1R, Nikon, Tokyo, Japan). The primers used for the vector construction are listed in supplementary Table S3.

238

239 **Protein extracts and immunoprecipitation assays**

240 The total proteins were extracted from *Nicotianna benthamiana* leaves using a membrane protein
241 extraction method with some modification.[55] The protein extracts were denatured and separated by
242 SDS-PAGE and then the gel was stained with Coomassie Brilliant Blue. For the Co-
243 immunoprecipitation (Co-IP) assay, TaNOX7$_{(1047\ bp)}$-GFP-tagged and TaCDPK13-6*Myc-tagged
244 proteins were detected by monoclonal anti-GFP antibody and anti-Myc antibody (SA003; ABclonal,
245 Wuhan, China), respectively. HRP goat anti-mouse IgG antibody (SA003; ABclonal) and antigen-
246 protein complex were detected using the ECL protein gel blot detection kit (GE Healthcare Life
247 Sciences, Beijing, China) and Light-Capture equipped with a CCD camera (ATTO, Shanghai, China)
248 as described by Kobayashi and others.[36] The primers used for the vector construction are listed in
249 supplementary Table S3.

250 # RESULTS

251 **Cloning of *TaNOX7* and analyses of its expression in wheat and rice**

252 Previously, we identified 46 members of NOX gene family in wheat genome,[23] however, no wheat
253 NOX members were further studied to clarify their exact functions in the plant development and/or
254 stress tolerance. In the present study, one wheat NOX gene, namely *TaNOX7-3A*, was cloned from
255 wheat cv. Chinese spring and characterized. There are three copies of TaNOX7 gene in wheat
256 genome, namely *TaNOX7-3A*, *TaNOX7-3B* and *TaNOX7-3D*, respectively. These three
257 homologuous genes shared similar gene structure and high identity in amino acids sequence (Fig.
258 S1). By using RNA-seq experiments on more than 100 wheat varieties, the main effectiveness of
259 the three homologuous genes in transcriptional expression was detected. As shown in Fig. 1A,

TaNOX7-3A (gene ID: AK334324) exhibited the highest expression level in wheat root, flag leaf and spike, showing that *TaNOX7-3A* might be the main effectiveness gene for TaNOX7 in wheat. Therefore, TaNOX7-3A was selected for further study. To simplify the phraseology, the gene is referred *TaNOX7* in the following experiments.

The amino acid sequence alignment showed that the TaNOX7 cloned here has high identity with HvRRboh2 (Hordeum_vulgare_MLOC_81745), OsRbohB (Os01g0360200), and AtRbohD (AT5G47910.1), and has all the conserved domains, namely NADPH_Ox (Pfam accession number PF08414), Ferric_reduct (PF01794), FAD_binding_8 (PF08022), and NAD_binding_6 domain (PF08022) as the typical NOXs possess (Fig. S2). Considering the fact that NOXs are the plasma membrane proteins,[5] we then examined the subcellular localization of TaNOX7 using a transient transformation system in both the protoplasts and leaf epidermal cells of *Nicotiana benthamiana* with AtCBL1n-mCherry served as a marker for plasma membrane protein location.[44] As expected, the TaNOX7-GFP fluorescence signals are well merged with those of AtCBL1n-mCherry at the plasma membranes (Fig. S3), confirming that TaNOX7 is also plasma membrane-located. These results suggest that a real NOX gene was successfully cloned from wheat.

As shown in Fig. 1B, *TaNOX7* is expressed in all tissues and at all developmental stages of wheat examined, although the expression exhibits tissue specificity at different stages. Compared with the level in roots of the seedlings at second-leaf stage, the transcriptional expression of *TaNOX7* is markedly higher in young spikes of the plant at booting stage. In addition, the expression of *TaNOX7* always keeps relative higher in spikes than that in leaves at the three reproductive growth stages, namely heading, flowering, and filling stages. Similar expression pattern for *TaNOX7* was also obtained from detection of β-glucuronidase (GUS) activity in *TaNOX7* promoter::GUS

transgenic rice plants (Fig. 1C). As can be seen, although the histochemical staining of GUS activity in transgenic plants was detected in all tissues examined, the strong staining was observed in germinating embryo (Fig. 1Cb), bud (Fig. 1Cc), young root (Fig. 1Cd), and young panicle (Fig. 1Cf-h). The predominant expression was found in the immature panicles at heading stage (Fig. 1Cg). With the grain development and getting mature, the GUS staining became weaker and weaker (Fig. 1Ch-j). All the results imply that TaNOX7 might play vital roles in the whole plant development, but preferentially in seed development.

Generation of transgenic plants and characterization of the phenotypes of transgenic plants

To further understand the function of TaNOX7, a series of transgenic plant lines were generated by introducing *TaNOX7* gene to the rice cultivar Nipponbare (WT) and an *OsNOX1*/*OsRbohB*-knockout mutant *osnox1* (the closest homologue of TaNOX7 in rice) as well as to the *Arabidopsis thaliana* wide-type and an *AtRbohD*-knockout mutant *atrbohd* (the closest homologue of TaNOX7 in *Arabidopsis*). Intriguingly, the *TaNOX7* transgenic rice plants showed two distinct phenotypes comparing with the WT. The rate of germination, root length, root hair density, and plant size in some lines are suppressed as similar to those in *osnox1*, while all these phenotypes in other lines are facilitated. For interpreting these phenotypes, semi-quantitative and quantitative RT-PCR assays were carried out to investigate the expression levels of *TaNOX7* and *OsNOX1* in these transgenic lines, respectively (Fig. 2Ad~f; Fig. S8B/C). As can be seen, although the transcripts of *TaNOX7* in all the transgenic rice plants are significantly higher than those in the WT and VC (transgenic lines for empty vector control), the transcripts of *OsNOX1* (*OsRbohB*) are markedly lower in the two

suppressed lines than the other plant lines. Considering the fact that introduced transgenes can often result in silencing of homologous endogenous genes as so called cosuppression,[56] the two suppressed lines obtained here were named as CS-2 and CS-3, respectively. While, the other overexpression lines were named as OE-2, OE-3, OE-5 and OE-6, respectively (Fig. 2A, 7A; Fig. S8). In addition, overexpression of *TaNOX7* in the *osnox1* mutant (the complementary lines, CO) restored the phenotypes of the mutant at the plant growth and fertility (Fig. S8A). As a whole, the morphology of the different rice lines exhibits a well correlation with the expression levels of *TaNOX7*, showing the pivotal roles of TaNOX7 in seed germination and seedling development.

Since ROS production is the basic function of NADPH oxidase enzymes, we then investigated whether differential expression of *TaNOX7* affected ROS production in rice under normal growth condition. Both the results obtained from histochemical staining and physiological measurement indicated that different transgenic plant lines generated different amounts of ROS (mainly O_2^- and H_2O_2). As shown in Fig. 2B and Fig. S8D/E, the CS lines and *osnox1* mutant exhibited quite lower O_2^- and H_2O_2 contents or production rate in both leaves and roots as compared to the WT and VC plants. On the contrary, the OE lines showed much stronger signals of DAB and NBT staining and higher contents and/or production rate of O_2^- and H_2O_2 than those of the WT and VC plants. Similar results were also obtained in the *TaNOX7* transgenic *Arabidopsis thaliana* (Fig. S6A/B). All these results exhibit a well correction between the *TaNOX7* transcriptional express levels and ROS production, suggesting that the roles of TaNOX7 in seed germination and plant development depend on its ROS producing activity (Fig. 2, 7; Fig. S8).

To further clarify the roles of TaNOX7-mediated ROS production in seed germination and plant development, we then treated the seeds and young seedlings of different transgenic plants with

exogenous H_2O_2. As shown in Fig. 3, the exogenous H_2O_2 application greatly influenced the seed germination rate and root development of the transgenic plants. The seed germination rate is obviously higher in the CS-2, CS-3 and *osnox1* plants than that in the WT and OE plants under exogenous H_2O_2 treatment even through it is much lower in those plants than the WT and OE under control condition (Fig. 3A ~ B). By contrast, the length of primary roots keeps no much difference between the different plant lines under the exogenous H_2O_2 treatment although it is markedly inhibited by the treatment. However, the adventitious root length and numbers are enhanced by the exogenous H_2O_2 treatment in all the transgenic plant lines with no remarkable differences existing between the plant lines (Fig. 3A~D). These results suggest that exogenous H_2O_2 application could, at least partly, restore the phenotype of the CS and *osnox1* plants in seed germination and root development, further demonstrating that the role of TaNOX7 in plant development depends on its ROS producing activity.

Drought tolerance of TaNOX7 transgenic rice plants

Since the differential expression of *TaNOX7* in rice greatly influenced the ROS production and its transcripts can be greatly upregulated under drought stress in wheat (Fig. S5), we then checked the possible function of this gene in plant drought tolerance. As can be seen in Fig. 4, similar to the *osnox1* mutant, the gene silence lines CS-2 and CS-3 are very sensitive to drought treatment as compared to the WT, VC and OE plants (Fig. 4A~C). After drought and rewatering, the survival rate of the CS plants is quite lower (25-30%) than that of the WT and VC lines (60-70%), whereas it is much higher in OE lines (80-90%) (Fig. 4D), showing that overexpression of TaNOX7 in rice enhanced the plant drought tolerance, which is closely related to the levels of its mediated ROS

production as described above. Furthermore, the CS plant lines and *osnox1* mutant exhibited much higher water loss rate than the WT whereas the OE plants are opposite (Fig. 4E), further indicating the roles of TaNOX7 in plant drought tolerance. The drought stress experiments were also carried out on *Arabidopsis* transgenic plants and a similar result was obtained (Fig. S6).

The interaction between TaNOX7 and TaCDPK13

To get more insights in the mechanism of TaNOX7 functions and activity regulation in wheat, the transcriptional expression patterns of *TaNOX7* and several CDPK genes including *TaCDPK2*, *4*, *13*, *14*, *17*, *20*, *21* and *22* were examined in 14 tissues of wheat from different development stages by qRT-PCR. As shown in Fig. S7, each gene examined has its unique expression pattern in wheat. Similar to *TaNOX7*, *TaCDPK2* and *4* are expressed in whole plant but no marked tissue-specificity. In terms of *TaCDPK14*, *17*, *20*, *21* and *22*, the dominant expression levels are mainly presented in leaves at early development stages. However, *TaCDPK13* is expressed in the whole plant but with peaking levels in spikes, which is much similar to that of *TaNOX7*, showing an obvious co-expression relationship between *TaNOX7* and *TaCDPK13* genes.

Then, we further analyzed the relationship between TaNOX7 and TaCDPK13 by employing different experimental approaches, including the firefly luciferase complementation imaging assay (LCI), bimolecular fluorescence complementation assay (BiFC) and coimmunoprecipitation (CoIP). As shown in Fig. 5A, strong fluorescent signals were detected in tobacco (*N. benthamiana*) leaves when *nLUC-TaNOX7* was co-expressed with *cLUC-TaCDPK13*. The interaction between TaNOX7 and TaCDPK13 was next verified by the BiFC assay since strong signals of YFP fluorescence were observed when *35S::TaNOX7-cYFP* was coexpressed with *35S::TaCDPK13-nYFP* in epidermal

cells of tobacco leaves (Fig. 5B). In addition, the interaction relationship of TaNOX7 and TaCDPK13 was further verified by the CoIP assay (Fig. 5C). As can be seen, a clear band of TaNOX7-GFP was observed in the TaCDPK13-MYC immunoprecipitates when the GFP-tagged protein was coexpressed with TaCDPK-MYC in tobacco leaves, showing that TaNOX7 physically interacts with TaCDPK13 *in vivo*.

Effect of TaNOX7 and TaCDPK13 interaction on ROS production and various aspects of the plant development

To dissect the biological significance of interaction between TaNOX7 and TaCDPK13, we at first used the *Agrobacterium tumefaciens*–mediated transient expression assay (agroinfiltration) to test whether transient co-expression of TaNOX7 with TaCDPK13 could affect the ROS production in plants. As shown in Fig. 5D, the DAB staining indicated that the reddish brown precipitates are much more in the areas of co-expression of *cLUC-TaCDPK 13* with *nLUC-TaNOX7* than the three controls in tobacco leaves, demonstrating that TaCDPK13 can promote ROS production by directly interacting with TaNOX7.

To further explore the physiological implications of TaNOX7 and TaCDPK13 interaction, the sophisticated expression profiles of *TaCDPK13* and *TaNOX7* in young spikes from 12 stages of wheat were investigated with the expression levels of the genes in flag leaves as the references (Fig. 6A). As expected, *TaNOX7* has an absolutely higher expression levels in the young spikes at all the examined developmental stages than that in the flag leaves. *TaCDPK13* exhibits a quite similar expression profile as *TaNOX7*, showing a very well coexpression relationship with *TaNOX7* during panicle development. In addition, *TaNOX7* and *TaCDPK13* also show very higher expression levels

392 in almost all the floral organs compared with those in the flag leaves (Fig. 6B). All the results
393 indicate that the interaction of TaNOX7 with TaCDPK13 may mainly function in the development
394 of spikes and floral organs, contributing to the fertility of the plant.
395
396 **Improvement of yield-component traits caused by TaNOX7 overexpression**
397 To further clarify the biological function of TaNOX7, the agronomic traits of *TaNOX7* transgenic
398 rice plants were comprehensively analyzed during the whole reproductive growth. As shown in Fig.
399 7 and Fig. S8, the differentially expression of *TaNOX7* in rice significantly influenced the plant
400 growth period and many other agronomic traits. The *TaNOX7*-overexpressing lines OE-5 and OE-6
401 show the shortest growth period (136~139 days) but the longest filling stage (35~36 days) among
402 the transgenic plants, followed by OE-2 and OE-3 with the middle growth period (145~147 days)
403 and the filling stage (25~28 days); while, the co-suppressed lines CS-2 and CS-3 have the longest
404 growth period (157~159 days) but the shortest filling stage (22~23 days). In contrast, the WT plant
405 possesses a 147-days growth period and a 24-days filling stage while the *osnox1* mutant has a 172-
406 days growth period and a 27-days filling stage (Fig. 7C). In addition, many yield-related traits
407 including the effective panicle number (Fig. S8F), percentage of effective panicle (Fig. 7Da), yield
408 per plant (Fig. 7Db), panicle length (Fig. S7H), percentage of seed setting (Fig. 7Dc), and thousand
409 kernel weight (Fig. 7Dd), show obvious higher in the *TaNOX7*-overexpressing lines (especially the
410 OE-5 and OE-6) but markedly lower in the CS plants and *osnox1* mutant as compared to those in
411 the WT. The OE plants also possess big panicles as compared to those of WT, CS lines and the
412 *osnox1* mutant (Fig. 7B). The phenotypes of the plants in these yielding characters are well
413 correlated with their *TaNOX7* expression and ROS producing levels (Fig. 7, S8). All these results

indicate that overexpression of *TaNOX7* in rice greatly improved the yielding traits of the plants and this, might be closely correlated with its function in ROS production.

DISCUSSION

In this study, a NADPH oxidase gene, namely *TaNOX7*, was cloned and characterized in wheat. Its encoding protein has the four conserved domains that the typical NOX/RBOH proteins have,[2, 38] and is located in the plasma membrane (Fig. S2, S3), demonstrating that the gene cloned here, do belongs to the NOX superfamily of plants. Nevertheless, the distribution of TaNOX7 on the plasma membrane is not uniform (Fig. S3), that is consistent with a previous study in which NOX/RBOH proteins were found to be presented on the plasma membrane by discrete dynamic spots with a highly heterogeneous diffusion coefficient.[32] Similar phenomenon was also observed on a rice NADPH oxidase OsRbohA.[17] In addition, it was reported that the homodimerization of OsRbohB is required for the interaction of the protein with a Rac GTPase.[57] Apparently, the homodimerization and dynamic state are the general form for the location of NOXs/RBOHs on the plasma membranes.

TaNOX7 participates in seed germination and seedling development by regulating ROS homeostasis

The spatio-temporal expression pattern showed that *TaNOX7* is expressed in almost all tissues and/or organs with dominantly transcripts in young spikes (Fig. 1B/D, 6, S7), implying its predominant roles in plant development, especially in young spikes. Many previous studies have shown that NOXs/RBOHs mediated ROS involves in various stages of plant development like seed germination, after-ripening, seedling growth, root development and so on.[58-60] In the present study,

436 we found that the seed germination rate, plant size and root length are greatly reduced in the *TaNOX7*
437 co-suppressed rice transgenic plants but increased in the overexpression lines. The expression level
438 of *TaNOX7* is closely associated with the seed germination rate and plant development as well as
439 the accumulation levels of O_2^- and H_2O_2 in transgenic plant lines (Fig. 2, S8A~E). These results
440 promote us to speculate that TaNOX7 may play pivotal roles in seed germination and plant
441 development by regulating the ROS production. In fact, increasing reports have indicated that ROS
442 produced by NADPH oxidases can promote GA biosynthesis, and subsequently GA induces and
443 activates NOXs for ROS production in aleurone cells, which induce α-amylase activity in aleurone
444 cells for seed germination.[58, 61] The functions of NOXs on regulating root development may also
445 depend on its ROS producing activity. A previous report indicated that AtRHD2 (an NADPH
446 oxidase) controls root development by making ROS that regulate plant cell expansion through the
447 activation of Ca^{2+} channels.[62]

448 The regulation of ROS to seed germination and root development seems bidirectional.
449 Although ROS (mainly H_2O_2) were found to facilitate seed germination,[63] root hair growth,[62] and
450 lateral roots[64] and adventitious roots development,[65] excess accumulation of them in seeds or in root
451 tops causes oxidative damage, which reduces germination ability[61] and root growth rate,[66]
452 respectively. Obviously, a critical balance between the production and elimination of ROS determine
453 the fate of the cells.[63] It was reported that, exogenous ABA mediated ROS accumulation produced
454 by AtRbohD and AtRbohF can positively or negatively affect the primary root growth, typically
455 depending on ABA concentrations: under high concentration, the increasing ROS repressed primary
456 root growth;[67] however, low ROS accumulation also reduced plant size and primary root length.[68]
457 Furthermore, exogenous H_2O_2 can reverse the suppressed root and root hair length to normal

458 phenotype in an *AtRbohC*-knockout mutant.[62] In the present study, as shown in Fig. 3, exogenous
459 H_2O_2 treatments significantly facilitate the seed germination rate of all the TaNOX7 transgenic rice
460 plants, especially in the gene silencing lines CS-2 and CS-3. While, the primary roots are retarded
461 eminently, but the adventitious roots (either the root length or number) are predominantly promoted
462 relative to that of the control groups. In a word, exogenous H_2O_2 can reduce the developmental gap,
463 which is due to the different level of endogenous ROS in different transgenic plant lines. This means
464 that the low expression of TaNOX7 mediated inhibition of seed germination and seedling
465 development could be eliminated by exogenous H_2O_2 application while the high expression of the
466 gene led facilitation of seed germination and seedling development could be suppressed by the
467 exogenous H_2O_2 treatment (Fig. 2, 3). Coincidentally, a similar case reported that the primary root
468 length is decreased and the lateral root number is increased in a dose dependent manner under
469 exogenous H_2O_2 in *Arabidopsis*.[64] Moreover, some other papers reported that the ROS produced by
470 AtRbohD and AtRbohF affect cytosolic Ca^{2+} levels and auxin sensitivity of roots, thus positively
471 regulating the ABA-inhibited primary root growth[67] and negatively modulating the lateral root
472 development by changing the peroxidase activity.[69] However, at high concentration (500 μM) of
473 exogenous H_2O_2 treatment reduced *Arabidopsis* root hair length.[70] Therefore, there must have a
474 ROS threshold interval in plants to maintain the normal physiological function, both above or below
475 the threshold are unfavorable to plants. Our results provide a solid evidence for this presumption.
476 To sum up, the results obtained here suggest that TaNOX7 is necessary for seed germination and
477 plant development by regulating ROS homeostasis.
478
479 **Overexpression of *TaNOX7* enhanced the fertility and drought-tolerance of**

transgenic plants

As shown in Figure 2, the rate of seed germination and root development were all positively correlated with ROS accumulation level and *TaNOX7* expression level. These results were sufficient to explain that TaNOX7 can regulate the vegetative growth of plant by regulate the ROS accumulation level. At the same time, the seedling growth status of plants will directly affect their fertility and tolerance to environmental stresses. In the present study, coinciding with their characteristics of seedling growth, the differential expressed *TaNOX7* transgenic plants also showed differential seed fertility and drought tolerance. Overexpression of *TaNOX7* in rice enhanced ROS accumulation, boosted plant fertility, increased panicle length, reduced the growing cycle and lengthened grain-filling duration (Fig. 7, S8), demonstrating that overexpression of this gene greatly improved yielding characters of the plants. Consistent with this, *TaNOX7* exhibited higher expression levels in young spikes and floral organs of wheat, implying its crucial roles in plant fertility and seeds development. The higher fertility owes much to healthy vegetative growth and longer reproductive growth. Coincided with this, the *TaNOX7*-overexpressing transgenic plants also showed shorten growth period of duration and relative longer reproductive growth stage (Fig. 7C). This is the first observation that NOXs/RBOHs might function in plant fertility and seed development although the functional mechanisms still remain under investigation.

Over-expression of *TaNOX7* in rice also greatly enhanced the tolerance of plants to drought stress, whereas suppression of its homologue *OsNOX1* or *AtRbohD* reduced the stress tolerance of plants (Fig. 4, S6), indicating that TaNOX7 also functions in plant stress tolerance. The roles of TaNOX7 in plant stress tolerance may also depend on its ROS producing activity. In fact, many important signaling pathways including Ca^{2+}, receptor-like protein kinases (RLKs), receptor-like

cytoplasmic kinases (RLCKs), calcium-dependent protein kinases (CDPKs),[71-73] botrytis-induced kinase1 (BIK1),[72] mitogen activated protein kinase (MAPK) cascades,[71, 74] open stomata 1 (OST1),[75] POP/RAC small GTPases, [76] and hormones (like ABA, JA, SA and ET),[9, 73, 77, 78] have been found participating in the activity regulation of NOXs/RBOHs to regulate ROS production for stress tolerance.[35] In our present study, we found that the drought tolerance of the *TaNOX7* transgenic rice is greatly consistent with the ROS production levels of the plants. The lower drought tolerance in the *TaNOX7* gene silencing lines is due to the low ROS level in these plants, which may block a stress related signal transduction and subsequently the intracellular resistance-related cascade reaction could not be motivated for the stress tolerance. While, overexpression of the gene enhanced ROS accumulation in plants and therefore improved the drought tolerance (Fig. 4, S6). However, the regulatory mechanism of TaNOX7 in ROS-producing needs further investigation.

The interaction between TaNOX7 and TaCDPK13 may contribute to the plant fertility and stress tolerance

It is well known that both NOX enzymes and CDPKs possess EF_hand domains, which are the crucial domains for Ca^{2+} binding. In fact, the roles of CDPKs in plant growth regulation and various stress responses are closely associated with NOX/RBOH-mediated ROS production in a Ca^{2+}-depended manner.[2, 79-81] In addition, both protein phosphorylation and Ca^{2+} show a synergistic effect on the activation of AtRbohH and AtRbohJ.[13] Therefore, as the primary Ca^{2+}-regulated kinases, CDPKs become the putative subjects for the phosphorylation of NOXs/RBOHs.[36, 37] All these results strongly suggest that phosphorylation of NOX/RBOHs in the Ca^{2+} dependent manner may be a general regulatory mechanism for the CDPK-mediated ROS-production. In the present study,

524 we found that TaCDPK13 could directly interact with TaNOX7 (Fig. 5A~C) and transient co-
525 expression of TaNOX7 with TaCDPK13 enhanced ROS production in tobacco leaves (Fig. 5D).
526 These results implied that TaCDPK13 can increase the activity of TaNOX7 and then enhanced the
527 production of ROS. Since the phosphorylation regulation of NOXs/RBOHs in CDPK-dependent
528 pattern widely exists in various species,[57, 82] we speculated that TaCDPK13 might also function on
529 the phosphorylation of TaNOX7 and thus regulate the ROS production for the plant development
530 and stress tolerance even though the mechanism of the interaction between TaNOX7 and
531 TaCDPK13 needs further verification.

532 As known to all, many genes have their specific expression pattern and functional preference.
533 For example, AtCDPK11 was found to participate in plant immune and abiotic stress signaling by
534 affecting transcriptional regulators as well as in pollen tube growth.[83, 84] While, OsCDPK9 plays a
535 positive role in drought tolerance and spikelet fertility.[85] Similarly, both *TaCDPK13* and TaNOX7
536 are all expressed in the whole plant but with peaking levels in spikes and floral organs (Fig. 6; Fig.
537 S7). At the same time, considering the differential characteristics of the TaNOX7 transgenic rice
538 plants on seedling growth, fertility, drought tolerance and ROS production, we speculate that the
539 interaction of TaNOX7 with *TaCDPK13* may play crucial function in the spike and flower organ
540 development at reproductive growth stage and therefore contributes to plant fertility by facilitating
541 ROS production.

542 As a whole, a novel NADPH oxidase homologue gene, *TaNOX7*, was identified and cloned
543 from wheat in this study. *TaNOX7* is expressed in whole plant with dominant transcripts in spikes
544 and floral organs of wheat. Overexpression of *TaNOX7* in rice led to more ROS production, faster
545 seed germination and seedling growth, higher drought tolerance, as well as shorter growth period

and improved yielding characters. TaNOX7 can directly interact with TaCDPK13, and plays vital roles in plant development, especially in fertility. Our study firstly reported that overexpression of an NADPH oxidase gene may facilitate yield production of crops with a shorten growth period, providing a promising and charming strategy to increase crop yields and stress tolerance using bioengineering technology.

AUTHOR INFORMATION

Correspondence author

*Kunming Chen

Tel.: +86-29-8703-1358; Fax: +86-29-8709-2262.

Email: kunmingchen@nwsuaf.edu.cn; kunmingchen@163.com.cn

ORCID

Kun-Ming Chen: http://orcid.org/0000-0002-0016-9995

Funding

This work was supported by the National Natural Science Foundation of China (grant no. 31770204 and 31270299) and the Program for New Century Excellent Talents in University of China (NCET-11-0440).

Notes

The authors declare that they have no conflict of interest.

SUPPORTING INFORMATION

Supplementary Figures

Figure S1. Comparative analysis of the protein conserved motifs and the amino acid sequences with three homologues of TaNOX7 (TaNOX7-3A, TaNOX7-3B and TaNOX7-3D). A. Alignment analysis of amino acid sequences for three homologues of TaNOX7. Amino acid sequences alignment analysis was performed using clustalx-2.1. B. The conserved domains of the protein TaNOX7. The logos of domain organization were obtained from EMBL-EBI.

Figure S2. Identification of *TaNOX7* and alignment analysis of its amino acid sequences with three other NADPH oxidases identified in other plants. Amino acid sequences alignment analysis was performed using clustalx-2.1 and GeneDoc 2.7.0. The blue/green/pink boxes represent that the conserved percent of the amino acid sequences between TaNOX7 and the three others (TaNOX7: AK334324; AtRbohD: AT5G47910.1; HvRRbohB2: ACB56482.1; OsRRbohB: XP_015620905.1) is 100%, 80% and 60%, respectively.

Figure S3. Subcellular localization of TaNOX7. The subcellular localization was analyzed by confocal microscopy using a transient transformation system with *Nicotiana benthamiana* as the materials. The top two panels show the analysis using tobacco protoplasts. Bars = 10 μm. The bottom two panels show the analysis using tobacco leaf epidermal cells. Bars = 50 μm. AtCBL1n-mCherry served as a marker for the plasma membrane localization of proteins.

Figure S4. Levels of ROS in root tips of the wild-type rice (WT), *TaNOX7*-transgenic lines and *OsNOX1*-knockout mutant *osnox1*. The ROS levels was visualized by confocal microscopy with fluorescence of 2, 7-dichlorodihydrofluorescein diacetate acetylester (H_2DCFDA; Sandalio et al. 2008). At least 10 of root tips from 4 day old plants were collected for the analysis. Relative fluorescence intensities were recorded from different positions along the central axes of the root tips

588 as marked by the rulers in the related pictures. Bars = 200 μm.

589 **Figure S5.** Inducible express pattern of *TaNOX7* under different biotic and abiotic stresses. The
590 expression profiles obtained from the database of TA_AFFY_WHEAT-0 as reported by
591 Genevestigator v3 Results were given as heat maps in green/red coding that reflect relative signal
592 values; where greener represents stronger down-regulated expression and redder represents stronger
593 up-regulated expression.

594 **Figure S6.** ROS production and drought tolerance of the *Arabidopsis* wild-type (WT, Columbia),
595 *TaNOX7*-transgenic plant lines, *AtRbohD*-knockout mutant *Atrbohd*, and complementary lines
596 (CO). A and B. DAB (A) and NBT (B) staining for detecting ROS (H_2O_2 and O^-_2) accumulation
597 levels in the 23 day old plants. C. 30 day old plants after drought treatment for 25 days. Data
598 represent similar results from more than three independent experiments.

599 **Figure S7**. Co-expression analysis of *TaNOX7* and *TaCDPKs* in 14 tissues of wheat by qRT-PCR.

600 **Figure S8.** Agronomic traits and ROS production of the wild-type rice (WT), *TaNOX7*-transgenic
601 lines, *OsNOX1*-knockout mutant *osnox1*, and complementary lines (CO). A. Phenotype of the
602 different type of plants at the heading stage. B. The relative expression levels of *OsNOX1* (the
603 homologue of *TaNOX7*) in the different type of plants. C. The relative expression levels of *TaNOX7*
604 in the different type of plants. D. The contents of O_2^- in the different type of plants. E. The contents
605 of H_2O_2 in the different type of plants. CO, the complementary lines complementing the mutant
606 *osnox1* with *TaNOX7*. F-I. Agronomic indexes of the different type of plants.

607

608 ## Supplementary Tables

609 **Table S1. The names of 100 wheat varieties**

610 **Table S2.** The information of the genes in this study

611 **Table S3.** The primers used in this study

612

613 ## Supplementary information SI for experimental program

614 **Plant materials and growth conditions**

615 **Total mRNA isolation and RT-PCR performance**

616 **Subcellular localization analysis**

617 **Transgenic plant generation**

618 **Detection of ROS production**

619 **GUS staining for the tissue/organ specific expression of *TaNOX7***

620 **Firefly luciferase complementation imaging (LCI) assay**

621 # REFERENCES

622 (1) Mittler, R.; Vanderauwera, S.; Suzuki, N.; Miller, G.; Tognetti, V. B.; Vandepoele, K.; Gollery, M.; Shulaev, V.;
623 Van Breusegem, F. ROS signaling: the new wave? *Trends Plant Sci.* **2011,** 16, 300-309.
624 (2) Yamauchi, T.; Yoshioka, M.; Fukazawa, A.; Mori, H.; Nishizawa, N.K.; Tsutsumi, N.; Yoshioka, H.; Nakazono,
625 M. An NADPH oxidase RBOH functions in rice roots during lysigenous aerenchyma formation under oxygen-
626 deficient conditions. *Plant cell* **2017,** 29, 775-790.
627 (3) Ying, W. NAD^+/NADH and $NADP^+$/NADPH in cellular functions and cell death: regulation and biological
628 consequences. *Antioxid Redox Signal*. **2008,** 10, 179-206.
629 (4) Muller, K.; Carstens, A. C.; Linkies, A.; Torres, M. A; Leubner-Metzger, G. The NADPH-oxidase AtrbohB
630 plays a role in *Arabidopsis* seed after-ripening. *New Phytol*. **2009,** 184, 885-897.
631 (5) Takeda, S.; Gapper, C.; Kaya, H.; Bell, E.; Kuchitsu, K; Dolan, L. Local positive feedback regulation determines
632 cell shape in root hair cells. *Science* **2008,** 319, 1241-1244.
633 (6) Chaouch, S.; Queval, G.; Noctor, G. AtRbohF is a crucial modulator of defence-associated metabolism and a
634 key actor in the interplay between intracellular oxidative stress and pathogenesis responses in *Arabidopsis*.
635 *Plant J.* **2012,** 69, 613-627.
636 (7) Xie, Y. J.; Xu, S.; Han, B.; Wu M. Z.; Yuan, X. X.; Han, Y.; Gu, Q.; Xu, D. K.; Yang, Q.; Shen, W. B. Evidence
637 of *Arabidopsis* salt acclimation induced by up-regulation of HY1 and the regulatory role of RbohD-derived
638 reactive oxygen species synthesis. *The Plant J.* **2011,** 66, 280-292.
639 (8) Maruta, T.; Inoue, T.; Tamoi, M.; Yabuta, Y.; Yoshimura, K.; Ishikawa, T.; Shigeoka, S. *Arabidopsis* NADPH
640 oxidases, AtrbohD and AtrbohF, are essential for jasmonic acid-induced expression of genes regulated by
641 MYC2 transcription factor. *Plant sci*. **2011,** 180, 655-660.
642 (9) Zhang, Y.; Zhu, H.; Zhang, Q.; Li, M.; Yan, M.; Wang, R.; Wang, L.; Welti, R.; Zhang, W.; Wang, X.

643 Phospholipase dalpha1 and phosphatidic acid regulate NADPH oxidase activity and production of reactive
644 oxygen species in ABA-mediated stomatal closure in *Arabidopsis*. *Plant Cell* **2009,** 21, 2357-2377.
645 (10) Denness, L.; McKenna, J. F.; Segonzac, C.; Wormit, A.; Madhou, P.; Bennett, M.; Mansfield, J.; Zipfel, C.;
646 Hamann, T. Cell wall damage-induced lignin biosynthesis is regulated by a reactive oxygen species- and
647 jasmonic acid-dependent process in *Arabidopsis*. *Plant physiol.* **2011,** 156, 1364-1374.
648 (11) Penfield, S.; Li, Y.; Gilday, A. D.; Graham, S.; Graham, I. A. *Arabidopsis* ABA INSENSITIVE4 regulates lipid
649 mobilization in the embryo and reveals repression of seed germination by the endosperm. *Plant cell* **2006,** 18,
650 1887-1899.
651 (12) Xie, H. T.; Wan, Z. Y.; Li, S.; Zhang, Y. Spatiotemporal production of reactive oxygen species by NADPH
652 oxidase is critical for tapetal programmed cell death and pollen development in *Arabidopsis*. *Plant cell* **2014,**
653 26, 2007-2023.
654 (13) Kaya, H.; Nakajima, R.; Iwano, M.; Kanaoka, M.M.; Kimura, S.; Takeda, S.; Kawarazaki, T.; Senzaki, E.;
655 Hamamura, Y.; Higashiyama, T.; Takayama, S.; Abe, M.; Kuchitsu, K. Ca^{2+}-activated reactive oxygen species
656 production by *Arabidopsis* RbohH and RbohJ is essential for proper pollen tube tip growth. *Plant cell* **2014,** 26,
657 1069-1080.
658 (14) Jimenez-Quesada, M.J.; Traverso, J.A.; Potocky, M.; Zarsky, V.; Alche, J.D. Generation of Superoxide by
659 Oerbohh, a NADPH Oxidase Activity During Olive (*Olea Europaea* L.) Pollen Development and Germination.
660 *Front. Plant Sci*. **2019**, 10, 1149.
661 (15) Yoshie, Y.; Goto, K.; Takai, R.; Iwano, M.; Takayama, S.; Isogai, A.; Che, F. S. Function of the rice $gp91^{phox}$
662 homologs OsrbohA and OsrbohE genes in ROS-dependent plant immune responses. *Plant Biotechnol.* **2005,**
663 22, 127-135.
664 (16) Nagano, M.; Ishikawa, T.; Fujiwara, M.; Fukao, Y.; Kawano, Y.; Kawai-Yamada, M.; Shimamoto, K. Plasma

membrane microdomains are essential for Rac1-RbohB/H-mediated immunity in rice. *Plant cell* **2016,** 28, 1966-1983.

(17) Wang, X.; Zhang, M. M.; Wang, Y. J.; Gao, Y. T.; Li, R.; Wang, G. F.; Li, W. Q.; Liu, W. T.; Chen, K. M. The plasma membrane NADPH oxidase OsRbohA plays a crucial role in developmental regulation and drought-stress response in rice. *Physiol. Plant.* **2016,** 156, 421-443.

(18) Wang S. S.; Zhu X. N.; Lin J. X.; Zheng W. J.; Zhang B. T.; Zhou J. Q.; Ni J.; PAN Z.C.; Zhu S.H.; Ding W.N. *OsNOX3*, encoding a NADPH oxidase, regulates root hair initiation and elongation in rice. *Biol. Plant.* **2018,** 4, 732-740.

(19) Rajhi, I.; Yamauchi, T.; Takahashi, H.; Nishiuchi, S.; Shiono, K.; Watanabe, R.; Mliki, A.; Nagamura, Y.; Tsutsumi N.; Nishizawa, N. K.; Nakazono, M. Identification of genes expressed in maize root cortical cells during lysigenous aerenchyma formation using laser microdissection and microarray analyses. *New Phytol*. **2011,** 190, 351-368.

(20) Nestler, J.; Liu, S.Z.; Wen, T.J.; Paschold, A.; Marcon, C.; Tang, H.M.; Li, D.L.; Li, L.; Meeley, R.B.; Sakai, H; Bruce, W.; Schnable, P. S.; Hochholdinger, F. Roothairless5, which functions in maize (Zea mays L.) root hair initiation and elongation encodes a monocot-specific NADPH oxidase. *Plant J.* **2014,** 79, 729-740.

(21) Cheng, X.; Li, G. H.; Manzoor, M. A.; Wang, H.; Abdullah, M.; Su, X. Q.; Zhang, J. Y.; Jiang, T. S.; Jin, Q.; Cai, Y. P.; Lin, Y. In silico genome-wide analysis of respiratory burst oxidase homolog (RBOH) family genes in five fruit-producing trees, and potential functional analysis on lignification of stone cells in Chinese white pear. *Cells* **2019**, 8, 520.

(22) Marino, D.; Andrio, E.; Danchin, E.G.; Oger, E.; Gucciardo, S.; Lambert, A.; Puppo, A.; Pauly, N. A *Medicago truncatula* NADPH oxidase is involved in symbiotic nodule functioning. *New Phytol*. **2011,** 189, 580-592.

(23) Hu, C. H.; Wei, X. Y.; Yuan, B.; Yao, L. B.; Ma, T. T.; Zhang, P. P.; Wang, X.; Wang, P. Q.; Liu, W. T.; Li, W. Q.; Meng, L. S.; Chen, K. M. Genome-wide identification and functional analysis of NADPH oxidase family genes in wheat during development and environmental stress responses. *Front. Plant Sci.* **2018,** 9, 906.

(24) Suzuki, N.; Miller, G.; Morales, J.; Shulaev, V.; Torres, M. A.; Mittler, R. Respiratory burst oxidases: the engines of ROS signaling. *Curr. Opin. Plant Biol.* **2011,** 14, 691-699. doi:10.1016/j.pbi.2011.07.014

(25) Dietz, K. J.; Mittler, R; Noctor, G. Recent progress in understanding the role of reactive oxygen species in plant cell signaling. *Plant Physiol.* **2016,** 171, 1535-1539. doi: 10.1104/pp.16.00938

(26) Adachi, H.; Nakano, T.; Miyagawa, N.; Ishihama, N.; Yoshioka, M.; Katou, Y.; Yaeno, T.; Shirasu, K.; Yoshioka, H. WRKY transcription factors phosphorylated by MAPK regulate a plant immune NADPH oxidase in *Nicotiana benthamiana*. *Plant cell* **2015,** 27, 2645-2663.

(27) Yao, Y.; He, R. J.; Xie, Q. L.; Zhao, X. H.; Deng, X. M.; He, J. B.; Song, L. L.; He, J.; Marchant, A.; Chen, X. Y.; Wu, A. M. ETHYLENE RESPONSE FACTOR 74 (ERF74) plays an essential role in controlling a respiratory burst oxidase homolog D (RbohD)-dependent mechanism in response to different stresses in *Arabidopsis*. *New Phytol*. **2017,** 213, 1667-1681.

(28) Zhang, M. X.; Chiang, Y. H.; Toruño, T. Y.; Dou, D. L.; Zhou, J. M.; Coaker, G. The MAP4 kinase SIK1 ensures robust extracellular ROS burst and antibacterial immunity in plants. *Cell Host & Microbe* **2018,** 24:1-13. doi: 10.1016/j.chom.2018.08.007.

(29) Ogasawara, Y.; Kaya, H.; Hiraoka, G.; Yumoto, F.; Kimura, S.; Kadota, Y.; Hishinuma, H.; Senzaki, E.; Yamagoe, S.; Nagata, K.; Nara, M.; Suzuki, K.; Tanokura, Masaru.; Kuchitsu, K. Synergistic activation of the *Arabidopsis* NADPH oxidase AtrbohD by Ca^{2+} and phosphorylation. *J. Biol. Chem.* **2008,** 283, 8885-8892.

(30) Kawarazaki, T.; Kimura, S.; Iizuka, A.; Hanamata, S.; Nibori, H.; Michikawa, M.; Imai, A.; Abe, M.; Kaya, H.; Kuchitsu, K. A low temperature-inducible protein AtSRC2 enhances the ROS-producing activity of NADPH oxidase AtRbohF. *Biochim. Biophys. Acta*. **2013,** 1833, 2775-2780.

(31) Li, L.; Li, M.; Yu, L. P.; Zhou, Z. Y.; Liang, X. X.; Liu, Z. X.; Cai, G. H.; Gao, L. Y.; Zhang, X. J.; Wang, Y. C.; Chen, S.; Zhou, J. M. The FLS2-associated kinase BIK1 directly phosphorylates the NADPH oxidase RbohD

711 to control plant immunity. *Cell Host & Microbe* **2014,** 15, 329-338.

712 (32) Hao, H. Q.; Fan, L. S.; Chen, T.; Li X. J.; He, Q. H.; Botella, A. M.; Lin, J. X. Clathrin and membrane
713 microdomains cooperatively regulate RbohD dynamics and activity in *Arabidopsis*. *Plant cell* **2014,** 26, 1729-
714 1745.

715 (33) Wong, H. L.; Pinontoan, R.; Hayashi, K.; Tabata, R.; Yaeno, T.; Hasegawa, K.; Kojima, C.; Yoshioka, H.; Iba,
716 K.; Kawasaki, T.; Shimamoto, K. Regulation of rice NADPH oxidase by binding of Rac GTPase to its N-
717 terminal extension. *Plant cell* **2007,** 19, 4022-4034.

718 (34) Daugaard, M.; Nitsch, R.; Razaghi, B.; McDonald, L.; Jarrar, A.; Torrino, S.; Castillo-Lluva, S.; Rotblat, B.; Li,
719 L.; Malliri, A.; Lemichez, E.; Mettouchi, A.; Berman, J. N.; Penninger, J. M.; Sorensen, P. H. Hace1 controls
720 ROS generation of vertebrate Rac1-dependent NADPH oxidase complexes. *Nat. Commun.* **2013,** 4, 2180.

721 (35) Hu, C. H.; Wang, P. Q.; Zhang, P. P.; Nie, X. M.; Li, B. B.; Tai, L.; Liu, W. T.; Li, W. Q.; Chen, K. M. NADPH
722 Oxidases: The vital performers and center hubs during plant growth and signaling. *Cells* **2020**, 9, 437.

723 (36) Kobayashi, M.; Ohura, I.; Kawakita, K.; Yokota, N.; Fujiwara, M.; Shimamoto, K.; Doke, N.; Yoshioka, H.
724 Calcium-dependent protein kinases regulate the production of reactive oxygen species by potato NADPH
725 oxidase. *Plant cell*, **2007,** 19, 1065-1080.

726 (37) Dubiella, U.; Seybold, H.; Durian, G.; Komander, E.; Lassig, R.; Witte, C.P.; Schulze, W.X.; Romeis, T.
727 Calcium-dependent protein kinase/NADPH oxidase activation circuit is required for rapid defense signal
728 propagation. *PNAS., U. S. A.* **2013,** 110, 8744-8749.

729 (38) Yu, H. X.; Xiao, A. F.; Dong, R.; Fan, Y. Q.; Zhang, X. P.; Liu, C.; Wang, C.; Zhu, H.; Duanmu, D. Q.; Cao, Y.
730 R.; Zhang, Z. M. Suppression of innate immunity mediated by the CDPK-Rboh complex is required for
731 rhizobial colonization in *Medicago truncatula* nodules. *New Phytol.* **2018,** 220: 425-434.

732 (39) Dmochowska-Boguta, M.; Nadolska-Orczyk, A.; Orczyk, W. Roles of peroxidases and NADPH oxidases in the

733 oxidative response of wheat (*Triticum aestivum*) to brown rust (*Puccinia triticina*) infection. *Plant pathology*
734 **2013,** 62, 993-1002. doi: 10.1111/ppa.12009
735 (40) International Wheat Genome Sequencing Consortium (IWGSC). Shifting the limits in wheat research and
736 breeding using a fully annotated reference genome. *Science* **2018,** 361, 661.
737 (41) Kim, D.; Langmead, B.; Salzberg, S. L. HISAT: a fast spliced aligner with low memory requirements. *Nat.*
738 *Methods* **2015,** 12(4), 357-360.
739 (42) Pertea, M.; Kim, D.; Pertea, G. M.; Leek, J.T.; Salzberg, S. L. Transcript-level expression analysis of RNA-seq
740 experiments with HISAT, StringTie and Ballgown. *Nat Protoc* **2016,** 11, 1650-1667.
741 (43) Chen, Y. F.; Li, L. Q.; Xu, Q.; Kong, Y. H.; Wang, H.; Wu, W. H. The WRKY6 transcription factor modulates
742 PHOSPHATE1 expression in response to low Pi stress in *Arabidopsis*. *Plant cell* **2009,** 21, 3554-3566.
743 (44) Batistič, O.; Waadt, R.; Steinhorst, L.; Held, K.; Kudla, J. CBL-mediated targeting of CIPKs facilitates the
744 decoding of calcium signals emanating from distinct cellular stores. *Plant J*. **2010,** 61, 211-222.
745 (45) Toki, S.; Hara, N.; Ono, K.; Onodera, H.; Tagiri, A.; Oka, S.; Tanaka, H. Early infection of scutellum tissue
746 with Agrobacterium allows high-speed transformation of rice. *Plant J*. **2006,** 47, 969-976.
747 (46) Clough, S. J.; Bent, A. F. Floral dip: a simplified method for Agrobacterium-mediated transformation of
748 *Arabidopsis thaliana*. *Plant J*. **1998,** 16, 735-743.
749 (47) Kumar, D., Yusuf, M. A.; Singh, P.; Sardar, M.; Sarin, N. B. Histochemical detection of superoxide and H_2O_2
750 accumulation in brassica juncea seedlings. *Bio-protocol*. **2014,** 4, e1108.
751 (48) Daudi, A.; O'Brien Jose A. Detection of hydrogen peroxide by DAB staining in *Arabidopsis* Leaves. *Bio-*
752 *protocol*. **2012,** 2, e263.
753 (49) Puyang, X.; An, M.; Han, L.; Zhang, X. Protective effect of spermidine on salt stress induced oxidative damage
754 in two Kentucky bluegrass (*Poa pratensis* L.) cultivars. *Ecotoxicol Environ Saf*. **2015,** 117, 96-106.

(50) Duan, Z.Q.; Bai, L.; Zhao, Z.G.; Zhang, G.P.; Cheng, F.M.; Jiang, L.X.; Chen, K.M. Drought-stimulated activity of plasma membrane nicotinamide adenine dinucleotide phosphate oxidase and its catalytic properties in rice. *J. Integr. Plant Biol.* **2009,** 51, 1104-1115.

(51) Asano, T.; Hayashi, N.; Kobayashi, M.; Aoki, N.; Miyao, A.; Mitsuhara, L.; Lchikawa, H.; Komatsu, S.; Hirochika, H.; Kikuchi, S.; Ohsugi, R. A rice calcium-dependent protein kinase OsCPK12 oppositely modulates salt-stress tolerance and blast disease resistance. *Plant J.* **2012,** 69:26-36.

(52) Liang, J. J.; Deng. G. B.; Long, H.; Pan, Z. F.; Wang, C. P.; Cai, P.; Xu, D. L.; Nima, Z. X.P; Yu, M. Q. Virus-induced silencing of genes encoding LEA protein in Tibetan hulless barley (Hordeum vulgare ssp. vulgare) and their relationship to drought tolerance. *Mol. Breeding* **2012,** 30, 441-451.

(53) Chen, H. M.; Zou, Y.; Shang, Y. L.; Lin, H. Q.; Wang, Y. J.; Cai, R.; Tang, X. Y.; Zhou, J. M. Firefly luciferase complementation imaging assay for protein-protein interactions in plants. *Plant physiol.* **2008,** 146, 368-376.

(54) Walter, M.; Chaban, C.; Schütze, K.; Batistic, O.; Weckermann, Katrin.; Näke, C.; Blazevic, D.; Grefen, C.; Schumacher, K.; Oecking, C.; Harter, K.; Kudla, J. Visualization of protein interactions in living plant cells using bimolecular fluorescence complementation. *Plant J.* **2004,** 40, 428-438.

(55) Liu, L. J.; Sonbol, F. M.; Huot, B.; Gu, Y. N.; Withers, J.; Mwimba, M.; Yao, J.; He, S. Y.; Dong, X. N. 2016, Salicylic acid receptors activate jasmonic acid signalling through a non-canonical pathway to promote effector-triggered immunity. *Nat. Commun.* **2016, 7**, 13099.

(56) Napoli, C.; Lemieux, C.; Jorgensen, R. Introduction of a Chimeric Chalcone Synthase Gene into Petunia Results in Reversible Co-Suppression of Homologous Genes in trans[J]. *Plant Cell* **1990,** 2(4):279-289.

(57) Oda, T.; Hashimoto, H.; Kuwabara, N.; Akashi, S.; Hayashi, K.; Kojima, C.; Wong, H.L.; Kawasaki, T.; Shimamoto, K.; Sato, M.; Shimizu, T. Structure of the N-terminal regulatory domain of a plant NADPH oxidase and its functional implications. *J. Biol. Chem.* **2010,** 285, 1435-1445.

(58) Kaur G,; Sharma A,; Guruprasad, K.; Pati, P. K. Versatile roles of plant NADPH oxidases and emerging concepts. *Biotechnol. Adv.* **2014,** 32:551-63.

(59) Montiel, J.; Arthikala, M. K.; Cardenas, L.; Quinto, C. Legume NADPH oxidases have crucial roles at different stages of nodulation. *Int. J. Mol. Sci.* **2016,** 17, 680.

(60) Li, W. Y.; Chen, B. X.; Chen, Z. J.; Gao, Y. T.; Chen, Z.; Liu, J. Reactive oxygen species generated by NADPH oxidases promote radicle protrusion and root elongation during rice seed germination. *Int. J. Mol. Sci.* **2017,** 18, 110.

(61) Kai, K.; Kasa, S.; Sakamoto, M.; Aoki, N.; Watabe, G.; Yuasa, T.; Iwaya-Inoue, M.; Ishibashi, Y. Role of reactive oxygen species produced by NADPH oxidase in gibberellin biosynthesis during barley seed germination. *Plant signaling & behavior* **2016,** 11, e1180492.

(62) Foreman, J.; Demidchik, V.; Bothwell, J. H.; Mylona, P.; Miedema, H.; Torres, M. A.; Linstead, P.; Costa, S.; Brownlee, C.; Jones, J. D. Reactive oxygen species produced by NADPH oxidase regulate plant cell growth. *Nature* **2003,** 422, 442-446.

(63) Neill, S. J.; Desikan, R.; Clarke, A.; Hurst, R. D.; Hancock, J. T. Hydrogen peroxide and nitric oxide as signalling molecules in plants. *J. Exp. Bot.* **2002,** 53, 1237-1247.

(64) Orman-Ligeza, B.; Parizot, B.; de Rycke, R.; Fernandez, A.; Himschoot, E.; Breusegem, F. V.; Bennett, M. J.; Périlleux, C,; Beeckman, T.; Draye, X. RBOH-mediated ROS production facilitates lateral root emergence in *Arabidopsis*. *Development* **2016,** 143, 3328-3339.

(65) Liao, W.B.; Zhang, M.L.; Huang, G. B.; Yu, J. H. Ca^{2+} and CaM are Involved in NO- and H_2O_2-induced adventitious root development in marigold. *J. Plant Growth Regul.* **2011,** 31, 253-264.

(66) Sun, C. L.; Liu, L. J.; Zhou, W. W.; Lu, L. L.; Jin, C. W.; Lin, X. Y. Aluminum induces distinct changes in the metabolism of reactive oxygen and nitrogen species in the roots of two wheat genotypes with different

aluminum resistance. *J. Agric. Food Chem*. **2017**, 65(43): 9419-9427.

(67) Jiao, Y.; Sun, L.; Song, Y.; Wang, L.; Liu, L.; Zhang, L.; Liu, B.; Li, N.; Miao, C.; Hao, F. AtrbohD and AtrbohF positively regulate abscisic acid-inhibited primary root growth by affecting Ca^{2+} signalling and auxin response of roots in *Arabidopsis*. *J. Exp. Bot.* **2013,** 64, 4183-4192.

(68) Kwak, J. M.**;** Mori, I. C.; Pei, Z. M.; Leonhardt, N.; Torres, M. A.; Dangl, J. L.; Bloom, R. E.; Bodde, S.; Jones, J. D. G. Schroeder, J. I. NADPH oxidase AtrbohD and AtrbohF genes function in ROS-dependent ABA signaling in *Arabidopsis*. *The EMBO Journal*. **2003,** 22, 2623-2633.

(69) Li, N.; Sun, L.; Zhang, L.; Song, Y.; Hu, P.; Li, C.; Hao, F. S. AtrbohD and AtrbohF negatively regulate lateral root development by changing the localized accumulation of superoxide in primary roots of *Arabidopsis*. *Planta* **2015,** 241, 591-602.

(70) Dunand, C.; Crevecoeur, M.; Penel, C. Distribution of superoxide and hydrogen peroxide in *Arabidopsis* root and their influence on root development: possible interaction with peroxidases. *New Phytol*. **2007,** 174, 332-341.

(71) Boudsocq, M.; Willmann, M. R.; Mccormack, M.; Lee, H.; Shan, L.; He, P.; Bush, J.; Cheng, S. H.; Sheen, J. Differential innate immune signalling via Ca^{2+} sensor protein kinases. *Nature* **2010,** 464(7287): 418-422.

(72) Kadota, Y.; Sklenar, J.; Derbyshire, P.; Stransfeld, L.; Asai, S.; Ntoukakis, V.; Jones, J. D.; Shirasu, K.; Menke, F.; Jones, A.; Zipfel, C. Direct regulation of the NADPH oxidase RBOHD by the PRR-associated kinase BIK1 during plant immunity. *Mol. Cell* **2014,** 54(1): 43-55.

(73) Mersmann, S.; Bourdais, G.; Rietz, S.; Robatzek, S. Ethylene signaling regulates accumulation of the FLS2 receptor and is required for the oxidative burst contributing to plant immunity. *Plant Physiol.* **2010,** 154(1): 391-400.

(74) Asai, S.; Ohta, K.; Yoshioka, H. MAPK signaling regulates nitric oxide and NADPH oxidase-dependent

oxidative bursts in *Nicotiana benthamiana*. *Plant Cell* **2008,** 20(5): 1390-1406.

(75) Sirichandra, C.; Gu, D.; Hu, H. C.; Davanture, M.; Lee, S.; Djaoui, M.; Valot, B.; Zivy, M.; Leung, J.; Merlot, S.; Kwak, J. M. Phosphorylation of the *Arabidopsis* AtrbohF NADPH oxidase by OST1 protein kinase. *FEBS Lett*. **2009,** 583(18): 2982-2986.

(76) Shin, L. J.; Huang, H. E.; Chang, H.; Lin, Y. H.; Feng, T. Y.; Ger, M. J. Ectopic ferredoxin I protein promotes root hair growth through induction of reactive oxygen species in *Arabidopsis thaliana*. *J. Plant Physiol*. **2011,** 168(5): 434-440.

(77) De Geyter, N.; Gholami, A.; Goormachtig, S.; Goossens, A. Transcriptional machineries in jasmonate-elicited plant secondary metabolism. *Trends Plant Sci*. **2012,** 17(6): 349-359.

(78) Durrant, W. E.; Dong, X. Systemic acquired resistance. *Annu. Rev. Phytopathol*. **2004,** 42: 185-209.

(79) Potocký, M.; Jones, M. A.; Bezvoda, R.; Smirnoff, N.; Zarsky, V. Reactive oxygen species produced by NADPH oxidase are involved in pollen tube growth. *New Phytol.* **2007,** 174, 742-751.

(80) Potocký, M.; Pejchar, P.; Gutkowska, M.; Jiménez-Quesada, M. J.; Potocká, A.; de Dios, A. J.; Kost, B.; Žárský, V. NADPH oxidase activity in pollen tubes is affected by calcium ions, signaling phospholipids and Rac/Rop GTPases. *J. Plant Physiol.* **2012,** 169:1654-1663.

(81) Boisson-Dernier, A.; Lituiev, D. S.; Nestorova, A.; Franck, C. M.; Thirugnanarajah, S.; Grossniklaus, U. ANXUR receptor-like kinases coordinate cell wall integrity with growth at the pollen tube tip via NADPH oxidases. *PLoS Biol*. **2013,** 11, e1001719.

(82) Ludwig, A. A.; Romeis, T.; Jones, J. D. CDPK-mediated signalling pathways: specificity and cross-talk. *J. Exp.Bot.* **2004,** 55, 181-188.

(83) Zhu, S. Y.; Yu, X. C.; Wang, X. J.; Zhao, R.; Li, Y.; Fan, R. C.; Shang, Y.; Du, S. Y.; Wang, X. F.; Wu, F. Q.; Xu, Y. H.; Zhang, X. Y.; Zhang, D. P. Two calcium-dependent protein kinases, CPK4 and CPK11, regulate

abscisic acid signal transduction in *Arabidopsis*. *Plant cell* **2007,** 19, 3019-3036.

(84) Zhao, L. N.; Shen, L. K.; Zhang, W. Z.; Zhang, W.; Wang, Y.; Wu, W. H. Ca^{2+}-dependent protein kinase11 and 24 modulate the activity of the inward rectifying K^+ channels in *Arabidopsis* pollen tubes. *Plant cell* **2013,** 25, 649-661.

(85) Wei, S.Y.; Hu, W.; Deng, X. M.; Zhang, Y. Y.; Liu, X. D.; Zhao, X. D.; Luo, Q. C.; Jin, Z. Y.; Li, Y.; Zhou, S. Y.; Sun, T.; Wang, L. Z.; Yang, G. X.; He, G. Y. A rice calcium-dependent protein kinase OsCPK9 positively regulates drought stress tolerance and spikelet fertility. *BMC Plant Biology*. **2014**, 14: 133.

FIGURE CAPTIONS

Figure 1. Tissue expression analysis of TaNOX7.

A. Expression levels of *TaNOX7* homologous copies in wheat by RNA-seq. Total RNA, used in RNA-seq experiments, are extracted from 100 varieties of wheat at inflorescence emergence stage. B. Tissue-specific expression analysis of *TaNOX7* in wheat by qRT-PCR with *TaActin1* (AB181991.1) and *TaGAPDH1* (ABS59297.1) as the internal controls. C. Spatial expression pattern of TaNOX7 in rice. Histochemical GUS assays were performed by using GUS staining (blue) in TaNOX7 promoter::GUS transgenic rice plants. a. Callus; b. Germinating seed; c. Bud; d. Seedling; e. Two-week old seedling; f. Seeds and panicles at booting stage; g. Flowers and panicles at heading stage; h. Panicles at milking stage; i. Seeds and panicles at dough stage; j. Seeds and panicles at full ripe stage.

Figure 2. Seed germination, root development, and ROS production in the wild-type rice, *TaNOX7*-transgenic lines and *OsNOX1*-knockout mutant *osnox1*.

A. Seed germination and root development in different transgenic lines. a. Seed germination after germinated 5 days. b. and c. Phenotypes of principal root, adventitious root and root hair of the young seedlings cultivated for 7 and 14 days, respectively. d. Expression of *TaNOX7* in the different type of plants analyzed by semi-quantitative PCR. e. Expression levels of *TaNOX7* in the different type of plants analyzed by qRT-PCR. f. Relative expression levels of *OsNOX1* in the different type of plants analyzed by qRT-PCR. B. ROS production detected by the histochemical staining and physiological measurement. a./b./e. H_2O_2 content detecting by 3,3'-diaminobenzimidine tetrachloride (DAB) staining in roots of 14-days old seedlings, principal roots of 4-days old

872 seedlings, and leaves from 7-days old seedlings, respectively. c./d./f. O_2^- content detecting by nitro
873 blue tetrazolium (NBT) staining in roots of 14-days old seedlings, principal roots of 4-days old
874 seedlings, and leaves from 7-days old seedlings, respectively. g. O_2^- production rate in the different
875 type of plants. The O_2^- production rate was detected with the XTT method (Duan et al., 2009).[47] h.
876 H_2O_2 content in the different type of plants. H_2O_2 content was detected by a Hydrogen Peroxide
877 Assay Kit (made in beyotime R technology). Leaves from 30-days old young seedlings were used
878 for the measurement of O_2^- production rate and H_2O_2 content. Values are means ± SD based on
879 three biological experiments with 3 to 5 technique replicates. Different letters indicate significant
880 differences determined by the Duncan (D) test.
881
882 **Figure 3. Effects of exogenous H_2O_2 treatment on the seed germination and root development**
883 **of the wild-type rice, *TaNOX7*-transgenic lines and *OsNOX1*-knockout mutant *osnox1*.**
884 A and B. Seed germination rate under 1.0 μM H_2O_2 treatment for 4 days. C and D. Root development
885 under H_2O_2 treatment (1.0 μM H_2O_2 for 4 d, and then 0.5 μM H_2O_2 for 3 d). Values are means ± SD
886 (n=20 plants) from three biological experiments. Different letters indicate significant differences
887 determined by the Duncan (D) test. CK, the control groups. VC, the vector control.
888
889 **Figure 4. Drought tolerance of the wild-type rice, *TaNOX7*-transgenic lines and *OsNOX1*-**
890 **knockout mutant *osnox1*.**
891 A. Phenotypes of the different type of plant lines before drought treatment (top panel), after
892 withholding water for 15 days (middle panel), and after rewatering for 10 days (bottom panel). 45
893 day old plants were used for drought stress treatment. B. Survival rate of the different type of plant

894 lines undergone drought and rewatering. Data are means ±SD (n = 50 plants) from more than three
895 independent experiments. Different letters indicate significant differences determined by the
896 Duncan (D) test. C. Water loss rate of the different type of plant lines. At least 6 leaves from two-
897 week old of seedlings for each plant line were used for the analysis. Three biological experiments
898 were performed for the examination. VC, the vector control.
899
900 **Figure 5. TaNOX7 interacts with TaCDPK13, which enhanced ROS production in plants.** A~C.
901 The interactions between TaNOX7 and TaCDPK13. A. Verification of protein interaction between
902 TaNOX7 and TaCDPK13 using the firefly luciferase complementation imaging (LCI) assay. B.
903 Bimolecular fluorescence complementation (BiFC) assay, showing the interactions between
904 TaNOX7 and TaCDPK13, respectively. C. The Co-Immunoprecipitation (Co-IP) assay, showing the
905 physically interactions between TaNOX7 and TaCDPK13 in vivo. D. Transient coexpression of
906 TaNOX7 with TaCDPK13 enhanced ROS production in the leaves of *N. benthamiana*. The level of
907 ROS accumulation was detected by 3, 3'-diaminobenzidine (DAB) dye. The DAB staining intensity
908 in situ ROS levels of agroinfiltrated tobacco leaves in each treatment was calculated based on the
909 stain intensity of the control "cLUC+nCLU". Bars annotated with different letters represent values
910 that are significantly different at $P \leqslant 0.05$ according to one-way ANOVA analysis.
911
912 **Figure 6. Expression profiles of T*aNOX7* and *TaCDPK13* in the spikes at different**
913 **developmental stages and floral organs at the heading stage of wheat.**
914 A. Expression profiles of the genes in the spikes at different development stages. B. Expression
915 profiles of the genes in different floral organs at the heading stage. The relative expression levels of

916 the genes in the spikes and floral organs were analyzed by qRT-PCR with using the expression levels
917 of the genes in flag leaves as the reference. Bars annotated with different letters represent values
918 that are significantly different at $P \leqslant 0.05$ according to one-way ANOVA analysis.
919
920 **Figure 7. Agronomic traits and yielding characters of the wild-type rice, *TaNOX7*-transgenic**
921 **lines and *OsNOX1*-knockout mutant *osnox1*.**
922 A. Phenotype of the different type of plants at the heading stage, showing the different maturing of
923 the panicles between the different plant lines. B. Phenotype of the mature panicles of the different
924 type of plants, showing the heavy panicles in the OE plants. C. The days of vegetative and
925 reproductive periods of the different type of plants. D. Yielding traits of the different type of plants.
926 At least 50 plants were used for the calculation of the percentage of effective panicles, weight of the
927 effective panicles per plant, and percentage of seed setting. For the analysis of thousand kernel
928 weight, three biological repeat experiments were performed. Bars annotated with different letters.

929 **TOC Graphical**

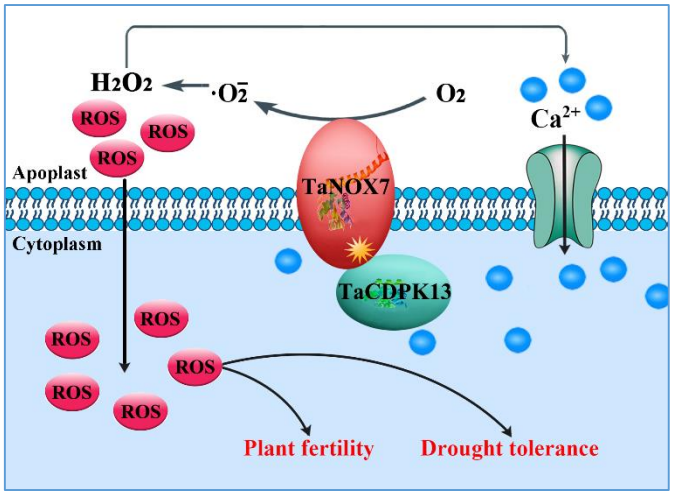

930

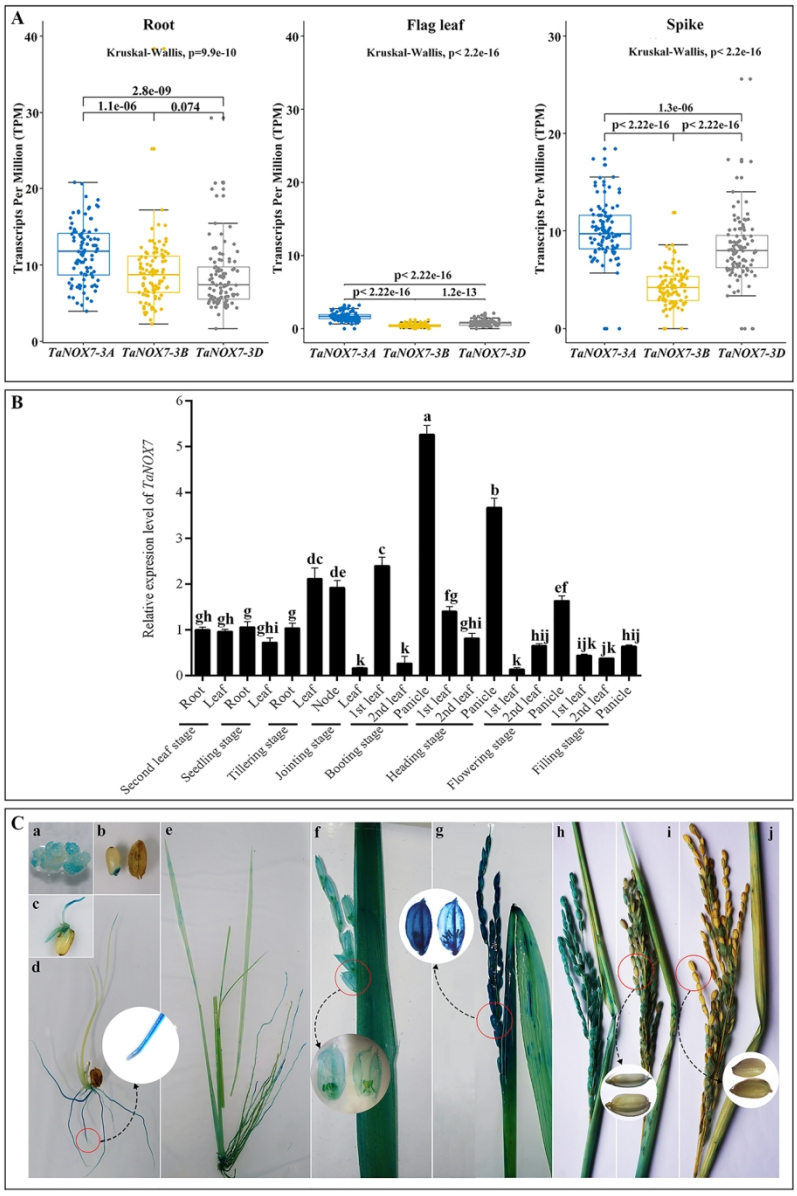

Figure 1. Tissue expression analysis of TaNOX7. A. Expression levels of *TaNOX7* homologous copies in wheat by RNA-seq. Total RNA, used in RNA-seq experiments, are extracted from 100 varieties of wheat at inflorescence emergence stage. B. Tissue-specific expression analysis of *TaNOX7* in wheat by qRT-PCR with *TaActin1* (AB181991.1) and *TaGAPDH1* (ABS59297.1) as the internal controls. C. Spatial expression pattern of TaNOX7 in rice. Histochemical GUS assays were performed by using GUS staining (blue) in TaNOX7 promoter::GUS transgenic rice plants. a. Callus; b. Germinating seed; c. Bud; d. Seedling; e. Two-week old seedling; f. Seeds and panicles at booting stage; g. Flowers and panicles at heading stage; h. Panicles at milking stage; i. Seeds and panicles at dough stage; j. Seeds and panicles at full ripe stage.

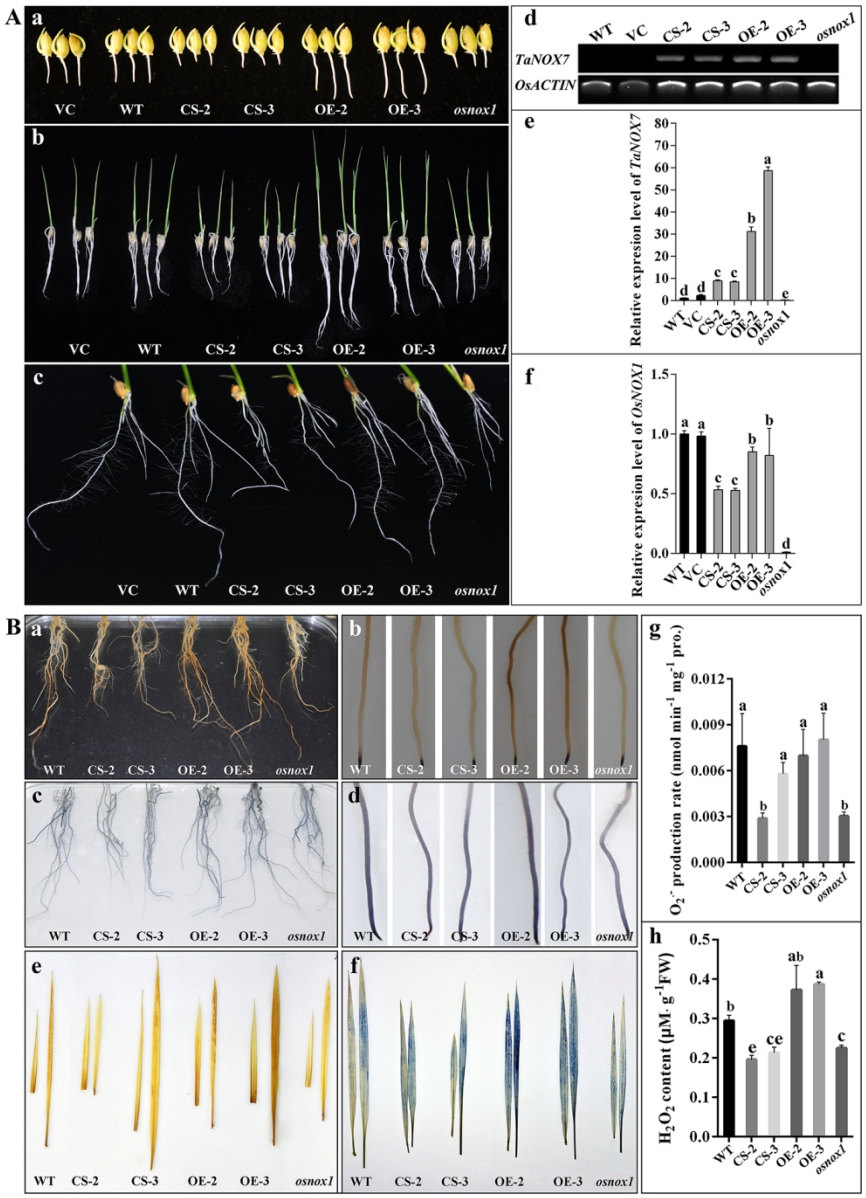

Figure 2. Seed germination, root development, and ROS production in the wild-type rice, *TaNOX7*-transgenic lines and *OsNOX1*-knockout mutant *osnox1*. A. Seed germination and root development in different transgenic lines. a. Seed germination after germinated 5 days. b. and c. Phenotypes of principal root, adventitious root and root hair of the young seedlings cultivated for 7 and 14 days, respectively. d. Expression of *TaNOX7* in the different type of plants analyzed by semi-quantitative PCR. e. Expression levels of *TaNOX7* in the different type of plants analyzed by qRT-PCR. f. Relative expression levels of OsNOX1 in the different type of plants analyzed by qRT-PCR. B. ROS production detected by the histochemical staining and physiological measurement. a./b./e. H_2O_2 content detecting by 3,3′-diaminobenzimidine tetrachloride (DAB) staining in roots of 14-days old seedlings, principal roots of 4-days old seedlings, and leaves from 7-days old seedlings, respectively. c./d./f. $\bullet O_2^-$content detecting by nitro blue tetrazolium (NBT) staining in roots of 14-days old seedlings, principal roots of 4-days old seedlings, and leaves from 7-days old seedlings, respectively. g. $\bullet O_2^-$ production rate in the different type of plants. The $\bullet O_2^-$ production rate was detected with the XTT method (Duan et al., 2009).47 h. H_2O_2 content

in the different type of plants. H_2O_2 content was detected by a Hydrogen Peroxide Assay Kit (made in beyotime R technology). Leaves from 30-days old young seedlings were used for the measurement of $\bullet O_2^-$ production rate and H_2O_2 content. Values are means ± SD based on three biological experiments with 3 to 5 technique replicates. Different letters indicate significant differences determined by the Duncan (D) test.

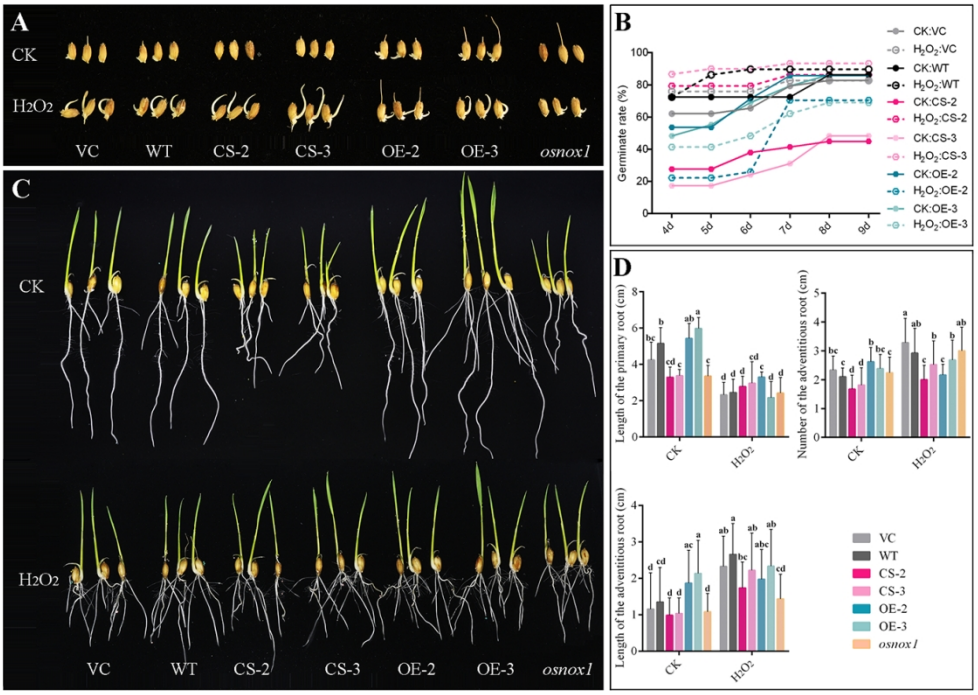

Figure 3. Effects of exogenous H_2O_2 treatment on the seed germination and root development of the wild-type rice, *TaNOX7*-transgenic lines and *OsNOX1*-knockout mutant *osnox1*. A and B. Seed germination rate under 1.0 μM H_2O_2 treatment for 4 days. C and D. Root development under H_2O_2 treatment (1.0 μM H_2O_2 for 4 d, and then 0.5 μM H_2O_2 for 3 d). Values are means ± SD (n=20 plants) from three biological experiments. Different letters indicate significant differences determined by the Duncan (D) test. CK, the control groups. VC, the vector control.

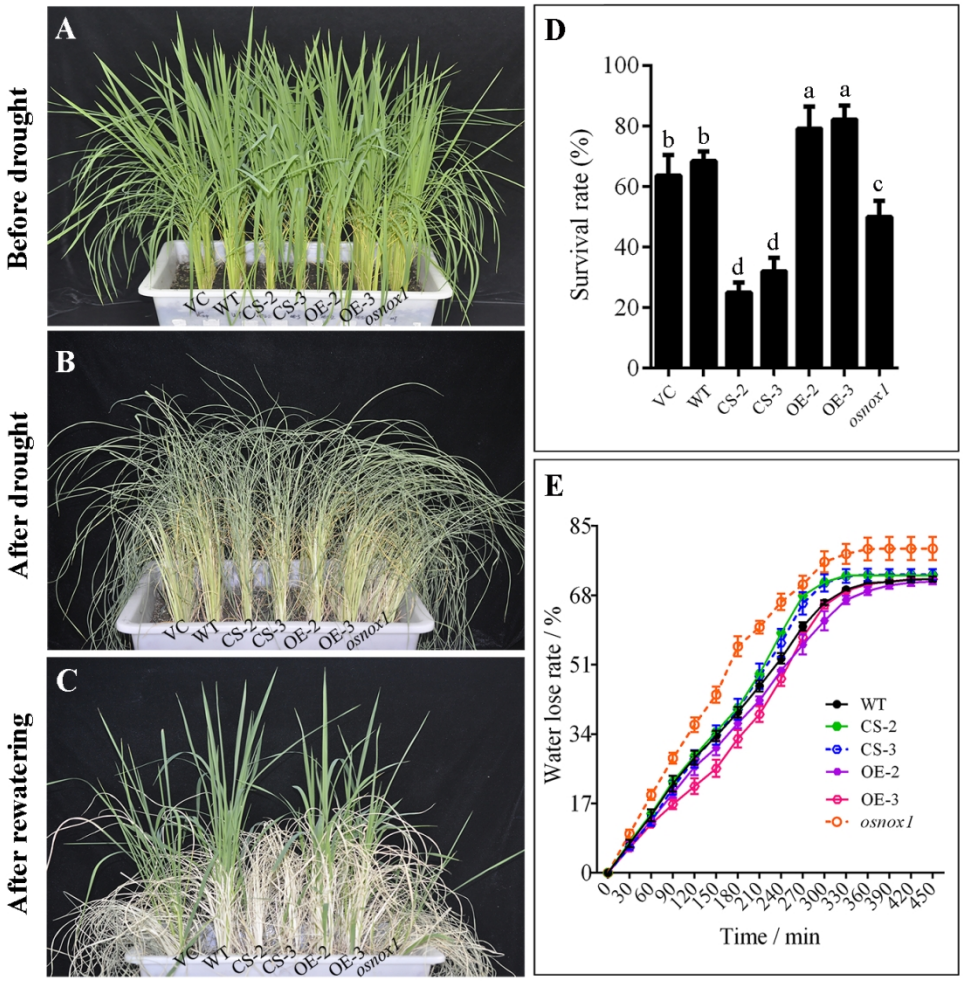

Figure 4. Drought tolerance of the wild-type rice, *TaNOX7*-transgenic lines and *OsNOX1*-knockout mutant *osnox1*. A. Phenotypes of the different type of plant lines before drought treatment (top panel), after withholding water for 15 days (middle panel), and after rewatering for 10 days (bottom panel). 45 day old plants were used for drought stress treatment. B. Survival rate of the different type of plant lines undergone drought and rewatering. Data are means ± SD (n = 50 plants) from more than three independent experiments. Different letters indicate significant differences determined by the Duncan (D) test. C. Water loss rate of the different type of plant lines. At least 6 leaves from two-week old of seedlings for each plant line were used for the analysis. Three biological experiments were performed for the examination. VC, the vector control.

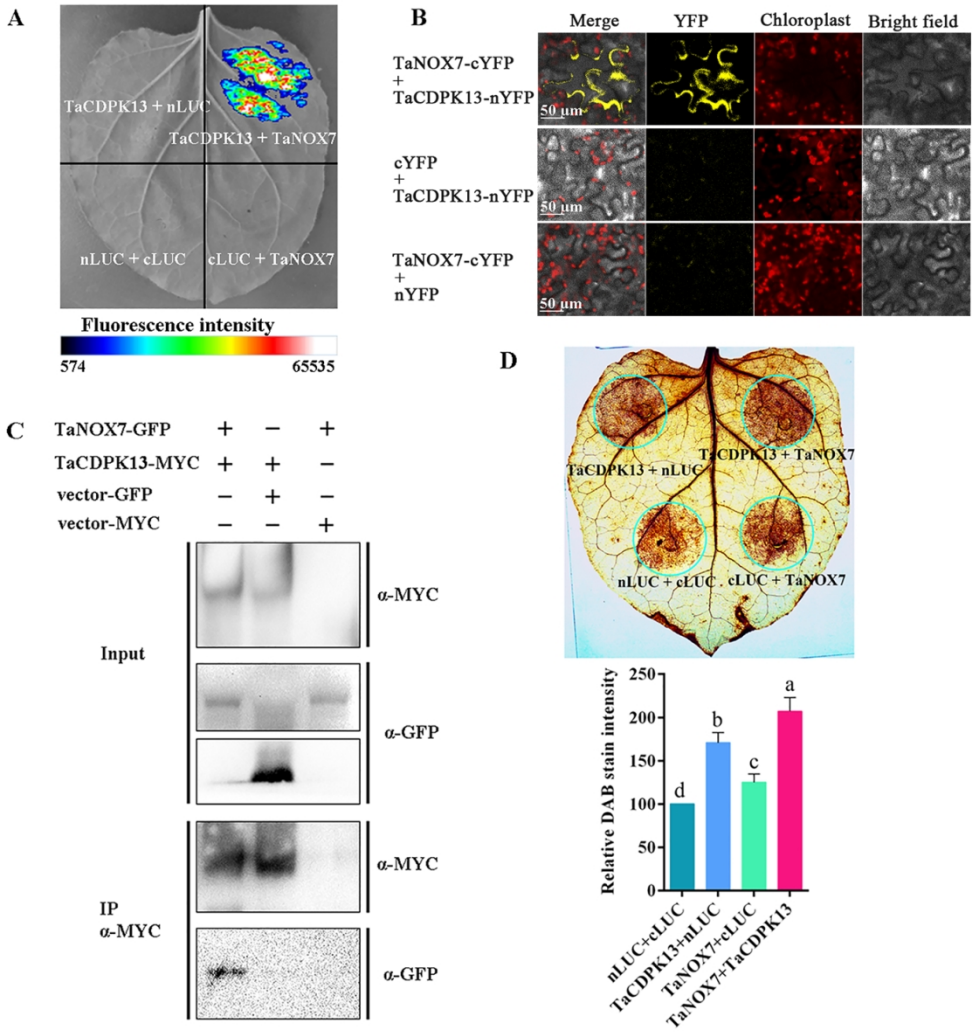

Figure 5. TaNOX7 interacts with TaCDPK13, which enhanced ROS production in plants. A~C. The interactions between TaNOX7 and TaCDPK13. A. Verification of protein interaction between TaNOX7 and TaCDPK13 using the firefly luciferase complementation imaging (LCI) assay. B. Bimolecular fluorescence complementation (BiFC) assay, showing the interactions between TaNOX7 and TaCDPK13, respectively. C. The Co-Immunoprecipitation (Co-IP) assay, showing the physically interactions between TaNOX7 and TaCDPK13 in vivo. D. Transient coexpression of TaNOX7 with TaCDPK13 enhanced ROS production in the leaves of N. benthamiana. The level of ROS accumulation was detected by 3, 3'-diaminobenzidine (DAB) dye. The DAB staining intensity in situ ROS levels of agroinfiltrated tobacco leaves in each treatment was calculated based on the stain intensity of the control "cLUC+nCLU". Bars annotated with different letters represent values that are significantly different at $P \leq 0.05$ according to one-way ANOVA analysis.

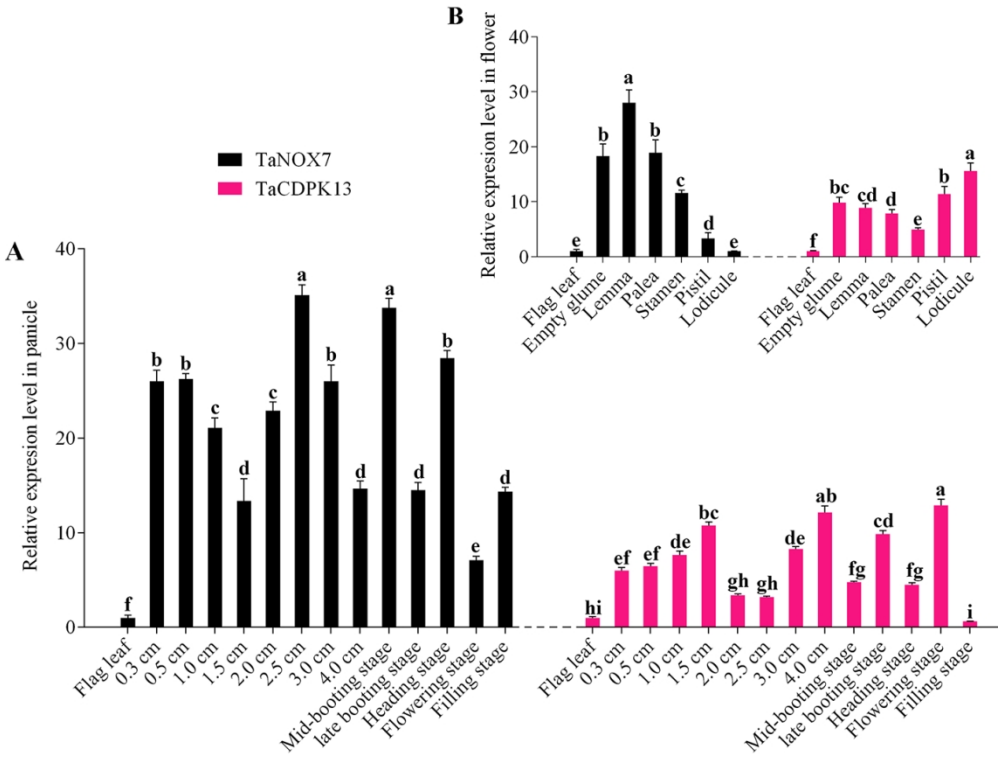

Figure 6. Expression profiles of TaNOX7 and TaCDPK13 in the spikes at different developmental stages and floral organs at the heading stage of wheat. A. Expression profiles of the genes in the spikes at different development stages. B. Expression profiles of the genes in different floral organs at the heading stage. The relative expression levels of the genes in the spikes and floral organs were analyzed by qRT-PCR with using the expression levels of the genes in flag leaves as the reference. Bars annotated with different letters represent values that are significantly different at P≤0.05 according to one-way ANOVA analysis.

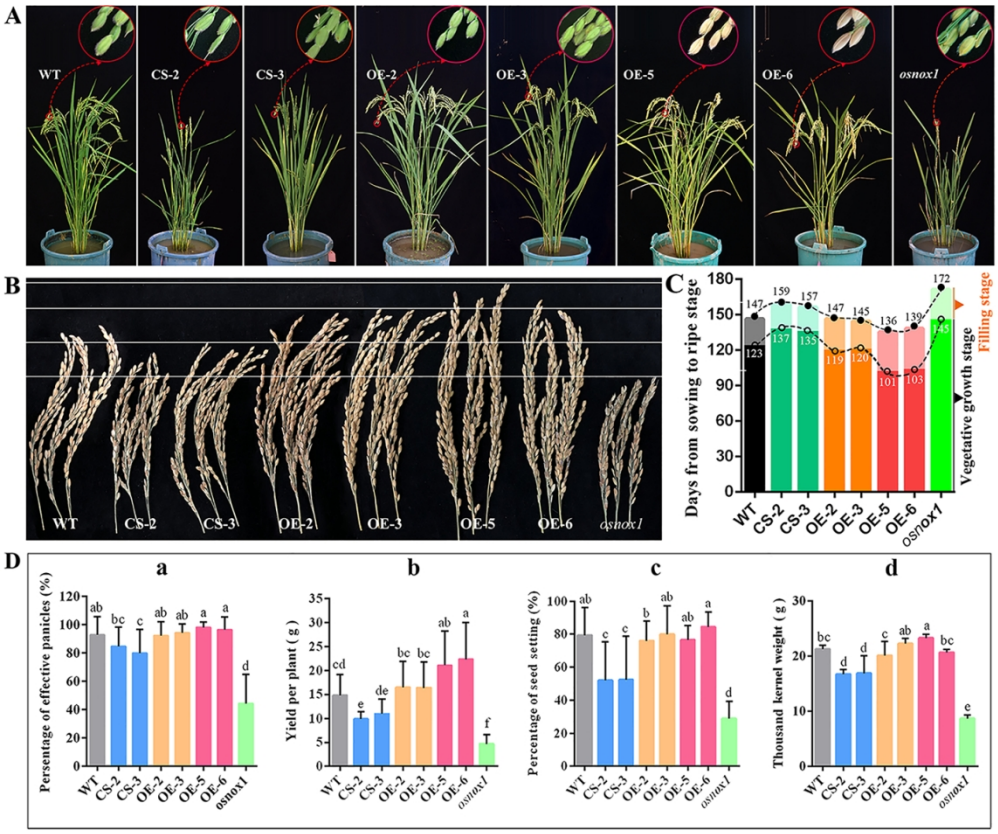

Figure 7. Agronomic traits and yielding characters of the wild-type rice, *TaNOX7*-transgenic lines and OsNOX1-knockout mutant *osnox1*. A. Phenotype of the different type of plants at the heading stage, showing the different maturing of the panicles between the different plant lines. B. Phenotype of the mature panicles of the different type of plants, showing the heavy panicles in the OE plants. C. The days of vegetative and reproductive periods of the different type of plants. D. Yielding traits of the different type of plants. At least 50 plants were used for the calculation of the percentage of effective panicles, weight of the effective panicles per plant, and percentage of seed setting. For the analysis of thousand kernel weight, three biological repeat experiments were performed. Bars annotated with different letters.